SURVEY OF CYLINDRICAL SHELL

RESPONSE AND WALL-PRESSURE

FLUCTUATIONS

by

Aouni A. Lakis and Samir S. Mohamed

RAPPORT TECHNIQUE NO EP 77-R-41

Département de Génie mécanique

Ecole Polytechnique

Montréal, Qué., Canada

Octobre 1977

CONTENTS

SURVEY OF CYLINDRICAL SHELL

RESPONSE AND WALL-PRESSURE

FLUCTUATIONS

by

Aouni A. Lakis and Samir S. Mohamed
Department of Mechanical Engineering
Ecole Polytechnique
Montreal, Que., Canada

SUMMARY

Thin-walled cylindrical shell response is reviewed in this report for various input excitations, with a special consideration to the response of cylindrical shells to subsonic turbulent boundary-layer fluctuations.

An analysis for predicting the cylindrical shell response to an arbitrary pressure field is derived.

In addition, the review of different investigations in determining the statistical properties of the wall-pressure fluctuations is performed.

Finally, a discussion of the shell response and comparison between various wall-pressure fluctuations investigations are also conducted.

1. INTRODUCTION

Most cylindrical shells are utilized in containing or conveying fluids, and this, to a certain extent, determines the classes of problems in which interest is focused. Thus, in addition to the determination of the vibration characteristics of the shells in vacuo, it is also of considerable pratical interest to predict the dynamical characteristics of shells containing either stationary or flowing fluid.

There are many ways in which the presence of the fluid may influence the dynamics of the shell. The free vibration characteristics of shells containing stationary gases at low pressure differ little from those in vacuo. In the case of a shell filled with compressible fluid, the compressibility of the fluid affects the effective stiffness of the system, in addition to the effects of straining of the shell by pressurization. If the density of the enclosed fluid is relatively high, as is the case with liquids, then the fluid exerts considerable inertial loading on the shell and results in diminishing the resonant frequencies significantly.

In the case of shells partially filled with liquid, on the other hand, free surface motions may be coupled to shell motions. This is of particular interest in liquid - propelled rockets where Large oscillations may develop - being usuallt referred to as "sloshing" -

in cases of proximity or coincidence of the natural frequencies of the free-surface motion and that of the shell. Also, there is a possibility of nonlinear coupling between the free-surface modes and the shell modes, resulting in subharmonic excitation of the former while the shell itself is oscillating at high frequencies. This phonemenon, however, is incompletely understood !

When the fluid is flowing, the shell is subjected to centrifugal forces and Coriolis - type forces. The former have the effects of diminishing the natural frequencies of the system, while the latter have a damping effects on vibration in cases where one end of the shell is free. The magnitude of these effects depends on the dimensionless flow velocity $\bar{U}_i$. Unless we are dealing with <u>rubber</u> shells, very heavy fluids or very high velocities, the values of $\bar{U}_i$ will be small and the effects of these forces will be correspondingly small $\begin{bmatrix} 12,61 \end{bmatrix}$. Thus for a steel cylindrical shell with $L/r = 26$ and $t/r = 0.023$ conveying air flow, $\bar{U}_i = 0.20$ corresponds to $U_x = 1000$ m/s. For this magnitude of flow velocity, the natural frequencies of the shell are found to diminish by only 3% as a result of the flow.

Similarly, in considering the response of cylindrical shells, considerable interest exists in the case where the excitation is transmitted through, or arises from, the contained fluid. This could take the form of pressure waves transmitted through the fluid; or if the fluid is flowing, the excitation could arise from gross pressure pertubations due to disturbances in the flow, or from boundary-layer pertubations.

Vibration caused by these pressure fluctuations may, in certain cir-
cumstances, cause fatigue failures of the structures involved.

The response of thin-walled cylindrical shells subjected to
boundary-layer fluctuations is studied by several investigators
applying various techniques such as "Green Function" with Cottis[4],
"Dira Delta Function" with Nasser [14] , "Joint-Acceptance Method"
with Clinch [6] , "Timoshenko Theory" with Magral [13] , Transfer
Function [22] , Beam theory [16] , Rayleigh method [15] , Energy
method [19] , Numerical Simulation and Fakker-Planch equations [9] ,
Forcing Function [8] and finally a hybrid classical-finite element
method by Lakis and Paidoussis [12] which is proved, the authors
believe, to be the most versatile.

Lakis and Paidoussis method [12] will be used by the authors to
predict the response of thin circular cylindrical shells either uniform
or axially non-uniform and subjected to subsonic turbulent two-phase
flow. It is a finite element theory, using cylindrical finite elements,
but the displacement functions are determined by using classical shell
theory, [12,33] . The random-pressure forces are lumped at the nodes
of the finite elements. Finally the cross-correlation spectral density
and the mean square value of the displacements of the shells are obtained
for an arbitrary pressure field and for a boundary-layer pressure field
in terms of the circumferential and lateral correlation functions of
the wall-pressure fluctuations. These statistical properties are deter-
mined experimentally; therefore an experimental air-water loop facility
is designed to suit our program purpose and permitting us of measuring

the space-time cross correlation functions and the r.m.s. response of the shell's wall.

The work presented in this report is an attempt to produce a review of thin cylindrical shells' response to an internal pressure, acoustic excitation, random pressure, internal and/or external flow. In addition the review of the measurements of the statistical properties of the wall-pressure fluctuations due to turbulent boundary-layer will be considered in details. Moreover, the role of surface wall-pressure fluctuations evaluations on wind panels, bodies of revolution and cylindrical shells with different mediums is alos discussed.

2. CYLINDRICAL SHELL RESPONSE

The response of shells to internal pressure, acoustic, random and turbulen boundary-layer excitations is reviewed in sections 2.1 to 2.4, followed by an outline, in section 2.5, of the hybrid classical finite element theory used by the authors to predict the shell response to turbulent two-phase flow excitation.

2.1 Shells response to internal pressure

The study of the dynamic response of a pressurized orthotropic cylindrical membrane has been presented by Dym [15] in both free and forced vibrations configurations. The effects of internal pressurization, inplane inertia and vibrations in the elastic constants are

also examined. Furthermore, Dym determined the effects of variations of the elastic constants on the free and forced motions of cylindrical membrane shells. His equations are based on the nonlinear shell theory, modified to delete the bending terms and to include orthotropic elastic constants. His solutions are in terms of the normal modes of free vibrations which are taken to be the Rayleigh type. Dym showed that the shell response is highly dependent on the internal pressure and on the relative magnitude of the applied load with respect to the internal pressure. In fact this work demonstrated clearly that the shell behavior is very significantly affected by the values of the various elastic constants and the ratio of the circumferential stiffness to the axial stiffness was found to be a particularly important parameter. Less importance has been attached to the relative magnitude of the inplane shear modulus. Finally he illustrated that the simplification of the analysis by the deletion of the inplane inertia terms induces little difference to the results of the forced vibration analysis.

In this regard, the frequencies and modes of free vibrations for various pressure vessels were conducted by Hamada [18], the different pressure vessels were changed according to the intensity of the internal pressure, and the fundemental equations were established for the statistical bending and vibration problems of the general axisymmetric loading and then subjected to some additional non-axisymmetric loading.

Hamada compared his numerical results with other experimental data and also compared the numerical results using Timoshenko's equations with those of his theory. The former comparison gave good agreement while the later showed slightly different results from Timoshenko's equations. However Hamada proved that his numerical method may solve comparatively easily the free vibration problems of the general axisymmetric shell subjected to pressure.

Concerning the principle of minimum total potential energy, applied by Vafakos [19], to obtain stresses and displacements for clamped, short oval cylindrical shells under hydrostatic pressure, the classical shell theory was employed in which buckling effects are not considered. Vafakos assumed a Fourier series for the deflections in the closed circumferential direction so that the partial differential equations of equilibrium are replaced by a set of ordinary differential equations.

Vafakos compared the energy solution with a simplified field approximation which can be considered an equivalent circular cylinder solution. Then he presented graphs of the significant stresses and displacements for the oval cylinders having major to minor axis ratios of 1.10, 1.30 and 1.50. Vafakos concluded that the maximum stresses and displacements increase significantly as the major to minor axis ratio increased.

An early investigation by Fung [20] studying the frequency spectra and vibration modes of thin-walled circular cylindrical shells subjected

to internal pressure remains one of the useful works in the field.
He showed that for very thin circular cylinders, the internal pressure has a significant effect on the natural vibration characteristics, particularly for cylinders having small length to diameter ratio and the mode associated with the lowest frequency is in general not the simplest mode. The exact number of circumferential modes associated with the lowest frequency depends upon the internal pressure and if this number is large, it decreases rapidly with the increasing pressure. At low pressure the fundamental frequency increases rapidly with increasing the internal pressure. Fung found out that at higher values of internal pressure the frequency increases with the increasing number of circumferential modes and the lowest frequency rises slowly with the internal pressure.

Experimental results on the frequency spectra, vibration modes and structural damping conducted by Fung for a series of thin cylindrical shells, showed agreement with the features predicted by Reissner's "shallow shell" vibration theory.

2.2 Shells response to acoustic excitation

Recently, the response of cylindrical shells due to random acoustic pressure input has been investigated by Hwang [17]. His analytical procedure was limited to a time-wise random pressure with defined spatial distribution. In general formulation, the pressure input may be both time-wise and space-wise random. Hwang's analysis applied the modal approach to define the shell response and also he considered the

interaction between the shell, the atmosphere and the shell structural damping as dispersion. He showed that in addition to the natural modes obtained by assuming a frictionless shell operating in a vacum, the impedance of the air column inside the cylindrical shell plays a significant role in determining the random acoustic response of the shell. He also described a formulation of the mean pressure spectrum inside the shell enclosure due to reverberation. The spectral data based on the presented analysis are generated for a typical cylindrical shells under random acoustic excitation.

Another investigation has been conducted on the response and equivalent force spectra by Kana [21] for random acoustic excitation of a cylindrical shells within a narrow band frequency of relative low-modal density. This approach involves the determination of theoritical structural admittances or transfer functions between response at some appropriate points and harmonic excitation at a single point. These functions can be expressed as series expansions of the normal modes of the system. Then by means of generalized harmonic analysis and superposition properties of linear random process theory, Kana obtained expressions relating the statistical properties of the response to the transfer functions, and to statistical properties of the excitations over the aggregate of the points in the area over which a distributed load acts. In general Kana found that a purely theoritical prediction of the response based on linear random process theory is severely limited because of the inability of currently available expressions for the transfer functions to account for various deviations which result principally from the imperfection and eccentricities in the cylinder.

However, good agreement is achieved between his measured response
and that calculated with measured transfer functions. He further in-
dicated that a rather coarse discrete representation of a continuous
by distributed excitation is possible.

2.3   Shells response to random excitation

The response of cylindrical shells due to random pressure exci-
tation is derived theoritically by several investigators with dif-
ferent techniques.

Recently, Thompson $\begin{bmatrix} 16 \end{bmatrix}$ applied an exact analysis using three
dimentional linear elasticity theory. It is developed for linear
elastic analysis of the response of pin-ended rod and tubes in a
stationary fluid medium, to random stationary homogeneous surface
pressure fluctuation. He presented a limited number of numerical
results, comparing the results of simple beam theory with the full
elastic analysis with respect to the prediction of response spectra
and mean square valves of radial and tangential surface displacement
and differential axial surface strains applying the local spectral
density in either band-limited white noise or Gaussian.

Similarly Magrab $\begin{bmatrix} 13 \end{bmatrix}$ studied the response due to forced harmonic
and random excitation of an elastic cylindrical shell sourrounded by

an inviscid fluid and concentrically contained by another thin elastic shell immersed in another inviscid fluid of finite extent. Magrab assumed that the shells motion can be described by the Timoshenko type shell theory which includes the effects of bending, transverse shear and rotatory inertia, the shell's motions are independent of the axial coordinates and the fluids motions are described by the classical curve equations. He considered two types of time varying functions for the applied forces, harmonic and stationary random functions. The field pressure is determined in the near and outer fluid.

On the other hand, Magrab derived expressions for the acoustic pressure at the outer surface of the inner shell; and the inner and outer surfaces of the outer shell along with the displacements at these surfaces. He also presented numerical results for the near and for field acoustic pressure.

A coupling between the Green function technique and Reissner shallow shell equation were applied by Cottis and Jasonides [4] to predict the response of a finite thin cylindrical shell to random pressure field. They applied the Reissner shallow shell equations of motions with the aid of the Green function solution assuming an homogeneous, isotropic and uniform wall thickness with two important approximations which are the independent displacement of the radial coordinates and the neglected longitudinal inertia terms.

An important result of Cottis analysis is the reduction of
the response integral representation to a single integral over
the unit circle in the complex plane.

Using assumed correlation functions for the pressure field,
Cottis and Jasonides derived a general expression for the space-
time correlation of the response; but they do not proceed to
evaluate the RMS and they do not undertake numerical solution
of the problem.

Similar application of the Green function has been conducted
by Cottis [22] for studying the general problem of the free and
forced vibrations of an orthotropic, finite shell within the limi-
tations of an approximate small deflection theory.

An application of the numerical simulation and Fokker-Planck
equations is presented by Nash [9], a large amplitude lateral
vibrations of thin, elastic, shallow shells subjected to random
excitation applied normal to the curves surface are examined with
several approximate techniques. The excitation is assumed to be
stationary, ergodic and Gaussian white noise. Nash applied the
numerical simulation of Rung and Kutta method and also Fokker-Planck
equations to determine the solution for the equations of motions
of the shallow shells, with various boundary conditions such as
simply-supported at both ends and clamped-clamped. He could obtain
a response of those shells in both cases of shallow and spherical
shells. He proved that the applied techniques are capable of pre-
dicting comparable estimates of the response as represented by the
central deflection of the shell.

A formal solution of the random responses of a thin-cylindrical shell has been performed by Wang [23] for simply supported thin shell subjected to non-axially symmetric concentrated stationary radial loading.

On the other hand, the Dirac delta technique is examined by Nasser [14] : a formulation of the second-order correlation function of the displacement field of a linearly elastic thin shell subjected to a random lateral pressure field is performed by him using a simply supported, shallow circular cylinder. Nasser derived an expression for the shell response using the Dirac delta function and Fourier transform to obtain the auto-correlation and the spectral density of the response and pressure field, respectively. He concluded that when the length of the shell becomes much larger than its radius, the length wise variation of the second order correlation function of the displacement field approachs a delta function while this field remains highly correlated in the circumferential direction.

2.4 Shells response to turbulent boundary-layer excitation

Prediction of the thin-walled cylindrical shell response to subsonic, turbulent boundary-layer, may be classified into i) purely theoritical-numerical research work such as Lakis [12,24]

and Corcos $\begin{bmatrix} 8 \end{bmatrix}$ and ii) mainly experimental one with some analytical

derivation as Clinch $\begin{bmatrix} 6,7 \end{bmatrix}$, Weyers $\begin{bmatrix} 25 \end{bmatrix}$ and Khosrovani $\begin{bmatrix} 26 \end{bmatrix}$. Each

of the mentioned investigators has different theoretical methods.

However, all the experimental techniques are based on the same ex-

perimental loop facility.

2.4.1   Theoritical investigations

Corcos $\begin{bmatrix} 8 \end{bmatrix}$ studied a random noise generated on the fuselage skin

of aircrafts by a turbulent boundary-layer. He applied through his

analysis the forcing function technique of several variables to de-

termine the response of linear systems to the random excitation,

assuming that the boundary-layer is locally homogeneous, the fuselage

skin is flat unlined and free from axial loads, and the cabin air

is bounded only by vibrating plates so that only the outgoing waves

are considered.

Corcos results showed that the sound pressure intensity is

proportional to the square of the free stream density, the square

of cabin air density and inversally proportional to the first power

of the damping constant and to the second power of the plate density

(cf. $\begin{bmatrix} 8 \end{bmatrix}$ p. 24). One of the main features of his results was that

the relevant quantities such as noise intensity are dependently non

dimensional numbers through which the boundary-layer and plate

properties enter as ratios.

Recently a general theory in the field of shells response has
been developed by Lakis and Paidoussis [12], to predict the r.m.s.
response of a non-uniform thin cylindrical shell subjected to an
arbitrary random pressure field. The theory is then specialized
to the case where the pressure field originates from the turbulent
boundary-layer of a subsonic internal flow. The basic formulation
is in terms of a finite-element theory but the displacement functions
are derived from Sanders'theory for cylindrical shells. The pressure
forces are lumped at the nodes of the finite elements. The cross-
correlation spectral density and the mean square value of the dis-
placements of the shell are obtained for an arbitrary pressure field
and for a boundary-layer pressure field.

More recently, this theory was extented i) to cases where the
shells are anisotropic [24] and especially for the case of shells
consisting of an arbitrary number of orthotropic layers; and ii)
to take into account the inertia, coriolis and centrifugal forces
of the moving fluid [61]

2.4.2   Experimental and theoritical investigations

One of the earliest investigation concerning the noise produced
by turbulent air flow adjacent to a flexible wall has been conducted
by Weyers [25]. He measured the spectrum and intensity of the
pressure field outside thin-walled cylinders containing fully deve-
loped turbulent pipe flow. In order to simplify the problem Weyers

assumed in his analysis that the motion of the surface of the cylindrical shell is described by a linear motion and the generation of random pressure field in the stationary medium is a linear radiation problem.

Weyers interpreted the measured spectra in relation to the elastic properties of the cylinders and the character of the turbulent fluctuations inside the flow. He found that the power spectrum of the pressure fluctuations in the stationary medium outside the vibrating cylinder is a function of the power spectrum of the wall pressure and the impedance of the thin wall cylinder. Also the natural frequencies of the cylinders could be identified and similarity parameters for the spectra were established. He also investigated the effect of cylindrical shell wall thickness on the spectrum and intensity óf the pressure fluctuations.

Weyers measurements, showed that the intensity of the external sound pressure field are scaled with the fifth power of the velocity at center of the pipe and also the intensity of the pressure fluctuations at the wall may be scaled with the fourth power of the velocity Hence, Weyers concluded that the ratio of the r.m.s. of wall pressure to the dynamic pressure is to be independent of the mach number and equal to a constant (0.0078).

A recent research work has been investigated by Khosrovani et al. [26] . They studied, experimentally and theoretically, the vibration of thin cylindrical duct due to internal random pressure field. Experimentally, the internal pressure cross-covariance coefficients were measured within a duct containing both a fully developed turbulent air flow and a sound field caused by a remote blower. Theoretically, Khosrovani assumed that turbulence convection is neglected, as being too high a frequency to influence the resulting significantly. Sound propagation is neglected and the pressure spectral density is presumed to be white noise. Applying these assumptions, the duct displacement response was derived by integration of the forcing and Green functions. This investigation is supported by a computer program.

In spite of his simplifications, Khosrovani measured displacement covariances showed a good agreement with those calculated. The predicted displacement spectral density is varying as w^{-3} with white noise excitation. He also observed that the dependence is $w^{-4.8}$ for the no-white noise forcing function with a frequency dependence near w^{-2}. However, he showed that the coefficients for spatial decay used in the forcing function model did not appear to depend on the flow speed.

Finally, Clinch [6] predicted experimentally and theoretically the vibration induced in thin-walled cylindrical pipes by the passage

of internal turbulent water flow. He derived a theoretical analysis based on the application of random vibration theory. A simply supported thin cylindrical shell was considered using Powells [27] joint-acceptance method, essentially by passing the need to introduce specific equations of motion. In his analysis, he assumed that the areas over which the wall pressure fluctuations correlated are small compared with pipe dimensions and more importantly, he considered the response only in high modes of the shell (where resonances are so close to one another that a continuous curve of response v.s. frequency may be assumed). With these assumptions and some others which are also made by Cottis [4], Clinch derived an expression for the root mean square of the wall displacement essentially as a function of frequency band width. Then he compared his theoretical results with his own experimental data which were conducted up to Reynold's numbers of 2×10^6. The average r.m.s. wall displacement plotted against frequency displays remarkably good agreement between theory and experiments (in the range of 100 - 1,000 Hz). It should be also pointed out that Clinch obtained experimentally some very useful correlation functions for the pressure field.

The most severe limitation of Clinch's theory is that is applies only for high mode numbers and frequencies (100 - 1,000 Hz).

It has been shown in Ref. [12] that the response at the high frequency range (100 - 1,000 Hz) is but a small part of the total. Thus, at the flow velocity of 248 in/sec the total mean square response is 3.2×10^{-8} in^2 whereas the high frequency response is 8×10^{-11} in^2, approximately, giving a ration of 20:1 for the corresponding r.m.s. values. The difference at higher flow velocities is even more pronounced. (Fig. 1).

2.5   Shells response to turbulent two-phase flow excitation

Lakis and Paidoussis theory [12] are considered in this development for the prediction of the shell response to turbulent two-phase flow. This theory predicts the shell's response with a minimum of limitations and also capable of analysing geometrically axially symmetric long or short, thin cylindrical shells which are not necessarily uniform and subject to any set of kinematic boundary condition including supports other than the two axial extremities of the shell. Only an outline of the theory is given here; for a detailed account the reader is referred to references [12,28,33,16] .

The equations of motion of the shell subjected to arbitrary load is given by

$$\left\{ [M] - [M_f] \right\} \{\ddot{y}\} + \left\{ [C] - [C_f] \right\} \{\dot{y}\} + \left\{ [K] - [K_f] \right\} \{y\} = \{F\}, \qquad (1)$$

where $\{y\}$ is a displacement vector, $[M]$ and $[K]$ are, respectively, the mass and the stiffness matrices of the shell in vacuo, and $[M_f]$, $[C_f]$ and $[K_f]$, represent the inertia, coriolis and centrifugal forces of the flowing fluid; $[C]$ is the damping matrix of the system and the external forces $\{F\}$ represent the internal random pressure field.

2.5.1 Determination of $[M]$ and $[K]$

The theory used to determine $[M]$ and $[K]$ is a hybrid of the finite element and classical shell theories. The finite element chosen is a cylindrical frustum (Fig. 2), and the displacement functions are determined by Sanders' theory for thin cylindrical shells $[3, 30]$.

In the continuum, we express the axial, circumferential and radial displacements of the middle surface of the shell by

$$\begin{Bmatrix} U(x, \phi) \\ W(x, \phi) \\ V(x, \phi) \end{Bmatrix} = \sum_{n=0}^{\infty} \begin{bmatrix} \cos n\phi & 0 & 0 \\ 0 & \cos n\phi & 0 \\ 0 & 0 & \sin n\phi \end{bmatrix} \begin{Bmatrix} u_n(x) \\ w_n(x) \\ v_n(x) \end{Bmatrix}, \qquad (2)$$

where u_n, w_n and v_n are the amplitudes of displacements associated with the nth circumferential wave number. Then for a specific n, the nodal displacement at node "i" (Fig. 2) is defined by

$$\{\delta_i\} = \left\{ u_{ni}, w_{ni}, (dw_n/dx)_i, v_{ni} \right\}^T. \qquad (3)$$

For a finite element with nodes i and j, the nodal displacement vector is $\{\delta_i, \delta_j\}^T$.

By substituting expressions (2) into Sanders' equations of motion and assuming

$$u_n(x) = Ae^{i\lambda x/r}, \quad v_n(x) = Be^{i\lambda x/r} \text{ and } w_n(x) = Ce^{i\lambda x/r} \tag{4}$$

and proceeding according to the finite element technique, the displacement functions were determined relating the continuum displacement to the nodal displacements.

Then the mass and stiffness matrices for one finite element $[m]$ and $[k]$, respectively, were obtained analytically by carrying out the necessary matrix operations and integrations. After lengthy manipulations, expressions for the general terms of $[k]$ and $[m]$ were obtained.

With $[m]$ and $[k]$ determined, the global mass and stiffness matrices for the whole shell $[M]$ and $[K]$, respectively, may be constructed by superposition in the normal manner. Each of these (square) matrices is of order 4 (N + 1) where N is the total number of finite elements. The interested reader is referred to Lakis and Paidoussis [28, 33] for details.

2.5.2 Inertia, $\left[M_f\right]$, Coriolis, $\left[C_f\right]$ and Centrifugal, $\left[K_f\right]$, forces of the moving fluid

When the fluid is flowing, the shell is subjected to inertia forces, centrifugal forces and coriolis-type forces coupled with the elastic deformation of its walls. It is assumed that the flow is potential and the fluid compressible. The conditions of impermeability of the surface of the shell and the dynamic condition of this surface which is given by Bernouilli's equation for distrubed motion, permit us to obtain the pressures of the fluid on the shell's walls. By carrying out the necessary matrix operations of the finite element method and integrating over x and φ we obtain the inertia, centrifugal and coriolis forces of the moving fluid as listed in reference [61].

The inertial loading exerted by the fluid on the shell results in diminishing the resonant frequency significantly. The centrifugal forces have also the effect of decreasing the natural frequencies of the system, while the coriolis-type pressure forces have a damping effect on vibrations in cases where one end of the shell is free. Unless we are dealing with very flexible shells, very heavy fluids, or very high velocities, the effects of the centrifugal and coriolis-type forces are relatively small [61].

2.5.3 Random pressure field induced by internal flow

In equation (1), the external forces $\{F\}$ represent the turbulent

random pressure fluctuations at the shell's walls resulting from the passage of fully-developed turbulent flow. The displacements are assumed small enough for the resultant forces to be normal to the shell's surface. It is also assumed that the pressure field is spatially continuous and that it has the properties of a weakly stationary, ergodic process. We further assume that the pressure drop in the length of the shell is sufficiently small for the mean pressure to be considered constant over the length of the shell. Finally, the continuous random pressure field of the deformable body is approximated by a finite set of discrete forces and moments acting at the nodal points $\begin{bmatrix} 32 \end{bmatrix}$.

As previously mentioned, the shell is divided into N finite elements, each of which is a cylindrical frustum. The position of the N + 1 nodal points may be chosen arbitrary (Fig. 2). Any pressure field is considered to be acting on an area S_e surrounding the node e of coordinate Z_e as shown in Figure 3 (a). We define the pressure distribution acting over this area S_e by two mutually perpendicular forces per unit length. We may write the actual resultant force per unit length,

$$F (x, \phi, t) = \sum_n f_{R_n} (x, t) \cdot \cos n\phi + \sum_n f_{C_n} (x, t) \cdot \sin n\phi \qquad (5)$$

where f_{R_n} and f_{C_n} are at a distance x_0 from the origin of the shell as shown in Figure 3 (a).

These two forces acting at point 'A' are transformed to two forces and one moment, M_r, acting at the node, e, as shown in Figure 3 (b). The external force vector associated with the n th circumferential wave number at a typical node, e, can now by written in the following form:

$$\left\{F(t)\right\}_e = \left[0, \int_{l_i'}^{l_i''} f_{R_n}(x_i, t)\, dx_i, \int_{l_j''}^{l_j''} (x_j - l_j)\, f_{R_n}(x_j, t)\, dx_j, \int_{l_i'}^{l_i'} f_{C_n}(x_p, t)\, dx_p \right]^T, \qquad (6)$$

where f_{R_n} and f_{C_n} are expressed in terms of the instantaneous pressure on the surface, p (x, ϕ, t), [12].

To obtain the mean square response, we proceed by first considering the free vibration of the conservative system and determining the natural frequencies Ω_i and the eigenvectros $\left[\Phi\right]_i$, i = 1, 2, ..., 4 (N + 1) - J, where J is the number of kinematic boundaries. We next form the modal matrix

$$\left[\Phi\right] = \left[\Phi_1, \Phi_2, \cdots, \Phi_{4\,(N+1)\,-\,J}\right], \qquad (7)$$

and define

$$\left\{y\right\} = \left[\Phi\right]\left\{Z\right\}. \qquad (8)$$

The equations of motion are decoupled by substituting equation (8) into (2) and assuming the damping matrix as linearly related to the mass and stiffness matrices. Finally, the cross-correlation spectral density and the mean square values of the displacements of

the shell are expressed in terms of correlation functions of the
pressure field; see equations (13) to (19) of reference $\begin{bmatrix}12\end{bmatrix}$:

$$\overline{y_g^2}(x_g, \phi_0, t) = \sum_{r=1}^{4(N+1)-J} \frac{\Phi_{qr}^2}{2\pi\Omega_r^4 M_r^2} \int_0^\infty \left|H_r(\Omega)\right|^2 \cdot$$

$$\cdot \left\{ \sum_{i=1}^{N+1}\sum_{u=1}^{N+1} \Phi_{ir}\Phi_{ur} \left|\int_{l_i'}^{l_i''} \int_{l_u'}^{l_u''} W_{fr}(\Omega;x_i,x_u)\,dx_i\,dx_u\right| + \right.$$

$$+ \sum_{i=1}^{N+1}\sum_{k=1}^{N+1} \Phi_{ir}\Phi_{kr} \left|\int_{l_i'}^{l_i''} \int_{l_k'}^{l_k''} (x_k - l_k) W_{fr}(\Omega;x_i,x_k)\,dx_i\,dx_k\right| +$$

$$+ \sum_{i=1}^{N+1}\sum_{v=1}^{N+1} \Phi_{ir}\Phi_{vr} \left|\int_{l_i'}^{l_i''} \int_{l_v'}^{l_v''} W_{frc}(\Omega;x_i,x_v)\,dx_i\,dx_v\right| +$$

$$+ \sum_{j=1}^{N+1}\sum_{u=1}^{N+1} \Phi_{jr}\Phi_{ur} \left|\int_{l_j'}^{l_j''} \int_{l_u'}^{l_u''} (x_j - l_j) W_{fr}(\Omega;x_j,x_u)\,dx_j\,dx_u\right| + \tag{9}$$

$$+ \sum_{j=1}^{N+1}\sum_{k=1}^{N+1} \Phi_{jr}\Phi_{kr} \left|\int_{l_j'}^{l_j''} \int_{l_k'}^{l_k''} (x_j - l_j)(x_k - l_k) W_{fr}(\Omega;x_j,x_k)\,dx_j\,dx_k\right| +$$

$$+ \sum_{j=1}^{N+1}\sum_{v=1}^{N+1} \Phi_{jr}\Phi_{vr} \left|\int_{l_j'}^{l_j''} \int_{l_v'}^{l_v''} (x_j - l_j) W_{frc}(\Omega;x_j,x_v)\,dx_j\,dx_v\right| +$$

$$+ \sum_{p=1}^{N+1}\sum_{u=1}^{N+1} \Phi_{pr}\Phi_{ur} \left|\int_{l_p'}^{l_p''} \int_{l_u'}^{l_u''} W_{fcr}(\Omega;x_p,x_u)\,dx_p\,dx_u\right| +$$

$$+ \sum_{p=1}^{N+1}\sum_{k=1}^{N+1} \Phi_{pr}\Phi_{kr} \left|\int_{l_p'}^{l_p''} \int_{l_k'}^{l_k''} (x_k - l_k) W_{fcr}(\Omega;x_k,x_p)\,dx_p\,dx_k\right| +$$

$$\left. + \sum_{p=1}^{N+1}\sum_{v=1}^{N+1} \Phi_{pr}\Phi_{vr} \left|\int_{l_p'}^{l_p''} \int_{l_v'}^{l_v''} W_{fc}(\Omega;x_p,x_v)\,dx_p\,dx_v\right| \right\} d\Omega,$$

where W_{fr} and W_{fc} are the cross-correlation spectral densities of the forces f_r and f_c, respectively; Φ_{qr} is the (qr)th element of the modal matrix $\left[\Phi\right]$, M_r is the element of the generalized mass matrix, Ω_r the r th natural frequency and H_r (Ω) is the magnification factor of the system defined by equation (16) of reference $\left[12\right]$.

The displacement power spectral density is of course real quantity. The pressure cross-correlation spectral density is a complex quantity; however its imaginary part vanishes as a result of the double area integration. Thus, the Re $\left[W_f\right]$'s are given as follows (see equations 20 to 25 of reference $\left[12\right]$):

$$\text{Re}\left[W_{fr}\ (\xi,\ \Omega)\right] = r^2 \int_0^{2\pi}\int_0^{2\pi} \Psi_{p\Omega}\ (\xi,0,0)\ \Psi_{p\Omega}\ (0,\eta,0)\ \overline{p_\Omega^2\ (t)}. \tag{10}$$

$$\cos\phi\ \cos\ (\phi+\eta)\ d\phi.\ d\ (\phi+\eta),$$

$$\text{Re}\left[W_{fc}\ (\xi,\ \Omega)\right] = r^2 \int_0^{2\pi}\int_0^{2\pi} \Psi_{p\Omega}\ (\xi,0,0)\ \Psi_{p\Omega}\ (0,\eta,0)\ \overline{p_\Omega^2\ (t)}. \tag{11}$$

$$\sin\phi.\ \sin\ (\phi+\eta)\ d\phi.\ d\ (\phi+\eta),$$

and

$$\overline{p_\Omega\ (x,\phi,t)\ p_\Omega\ (x+\xi,\ \phi+\eta,\ t)} = \Psi_{p\Omega}\ (\xi,0,0)\ \Psi_{p\Omega}\ (0,\eta,0)\ \overline{p_\Omega^2\ (t)},$$

where r is the radius of the shell; the quantities $\Psi_{p\Omega}\ (\xi,0,0)$ and $\Psi_{p\Omega}\ (0,\eta,0)$ are respectively, the axial and circumferential correlation functions of the pressure field; $p_\Omega^2\ (t)$ is the mean square of the pressure

fluctuations; $\xi = \left| x_i - x_j \right|$, $\eta = r(\phi_j - \phi_j)$ Ω is the center frequency and $p_\Omega (x,\phi,t)\, p_\Omega (x+\xi,\, \phi+\eta,\, t)$ is the cross-correlation function.

Equations (9), (10) and (11) together express the response of the shell, $y_q^2 (x_q,\, \phi_q,\, t)$, in terms of the pertinent correlations - $\Psi(\xi,0,0)$, $\Psi(0,\eta,0)$ and $p_\Omega^2(t)$-of an arbitrary homogeneous random pressure field. This r.m.s. response is calculated for each circumferential wavenumber, n, and the total response may then be found by summing over n.

Equation (9) gives the r.m.s. response in terms of quite general correlation functions which are to be determined experimentally for each particular case of flow. We are interested in a random pressure field induced by a turbulent two-phase flow; so an experimental loop facility is designed to measure the correlation functions of such flow.

In the case of subsonic boundary-layer pressure fluctuations, the circumferential and lateral correlation functions have been examined experimentally by Bakewell et al. [44] and Clinch [48]. Bakewell measured and derived expressions for the axial and circumferential correlation functions in experiments with air flowing in cylindrical pipe. Clinch measurements in water proved that these expressions are approximately the same for different fluids at the same Strouhal number. Upon using the experimentally based relations of Bakewell et al. the r.m.s. response is obtained at each node of

the shell $\left[12\right]$. The aim of the next chapter is to review the different experimental investigations in the field of wall-pressure fluctuations.

3.   THE FLUCTUATING WALL-PRESSURE FIELD OF A TURBULENT BOUNDARY-LAYER

Wall-pressure fluctuations produced by a turbulent boundary-layer have been the subject of many investigators. Early experimental work was, on the whole confined to measurements of the root mean square and frequency spectra of the wall-pressure, and in many cases the instrumentation available did not give an adequate coverage of the band-width of the fluctuations. Moreover recently the development of miniature, piezoelectric pressure transducers and the extensive use of correlation techniques has led to a much more detailed examination of the wall-pressure field and its relation to turbulent velocity fluctuations in the boundary-layer.

Our review will cover the experimental investigations of the wall-pressure fluctuations of panels, body of revolution and cylindrical shells. The transducers size, shape and their orientation are also investigated.

The statistical properties of wall-pressure fluctuations are analyzed in references $\left[12,34,39,54 \text{ and } 60\right]$. The instrumentations used for recording and analysing the statistical properties

of pressure fluctuations are basically the same for several investi-
gations (Fig. 4):   Each pair of transducers is connected to pream-
plifier and to analog correlator through band pass filter, variable
gain amplifier, octave band analyzer, variable time delay, d.c.
millivoltmeter and finally to cross-correlation data output.   In
addition, through the octave band analyzer, the signal is connected
to true r.m.s. voltmeter and to the power spectrum data output.

3.1   Wall-pressure fluctuations at panel

One of the earliest investigation has been done by Tack et al.
[35] studying the correlation properties of turbulent wall-pressure
fluctuations.   Experimentally, he used a test section of rectangu-
lar cross section with inside dimensions 8 by 2.9 cm and 76.2 cm
long.   Its sides are constructed of 1/2 inch plexiglass, applying
flexible microphone porbe tube to permit two condenser microphones
to measure the instantaneous pressure fluctuations with the assump-
tion that the pressure field is adequately described by a random
process which is stationary and homogeneous and the correlation
decays in time as it is convected in the flow direction.

Tack found that both mean eddy size and mean eddy lifetime
determined by averaging over broad frequency bands do not contain
sufficient information to describe accurately the high frequency and the
turbulent power spectrum.   However by measuring eddy sizes and lifetime

over narrow bands frequencies, it appears possible to construct mathematically models of the turbulent pressure correlation which are sucessful in predicting the turbulent power spectrum over the frequency band of interest. Tack et al. measured the longitudinal spatial pressure correlations, Fig. 5a, where time delay is zero and the longitudinal space-time pressure correlations, Fig. 5b, for critical time delay between signals at flow speed of 40 m/sec and over a narrow band centered at a frequency of 450Hz. They further assumed suitable models for the spatial pressure correlations:

$$\overline{p\ (x,t)\ p\ (x\text{-}\xi,t)} = \overline{p^2\ (x,t)}\left[\sin\ (K_1 \xi)/K_1 \xi\right],\tag{12}$$

and for the space-time correlation function:

$$\overline{p\ (x,t)\ p\ (x\text{-}\xi,\ t\text{-}\zeta)} = \overline{p^2\ (x,t)}\left[\sin\ K_1 (\xi\text{-}U_c\zeta)/K_1 (\xi\text{-}U_c\zeta)\right]e^{-|\zeta|/\Theta_1},\tag{13}$$

where $\xi = \Delta x$, K_1 is constant over a particular frequency band, U_c is the convection velocity, ζ is time delay and the quantity Θ_1 is the time rate of decay of coherence.

The two parameters K_1 and Θ_1 are functions of both velocity and frequency; it is possible to predict their values from directly measurable properties of the turbulent boundary-layer such as boundary-layer thicknesses, free stream velocity, temperature, fluid density and turbulent power spectrum. They also suggested a numerical value predicted by Willmarth [43] for the mean square pressure, $\overline{p_\Omega^2}\ (t)$.

Bull $\begin{bmatrix} 36 \end{bmatrix}$ studied the wall-pressure fluctuations produced by a turbulent boundary-layer and determined its statistical properties in conditions covering various values of boundary-layer thickness and flow speeds. The measured quantities include r.m.s. pressures, frequency spectra, longitudinal and lateral space-time correlations, in both broad bands and narrow frequency bands.

The wind tunnel test section was of 9 X 6 inches and subsonic test section of 10 ft long followed by a supersonic section of 6 ft long. The measurements of the fluctuating pressure were made with piezo-electric transducers, set flush in the wind tunnel wall. Some experimental values of the space-time correlation between wall-pressure fluctuations and turbulent velocity fluctuations at various positions of the boundary-layer are also determined.

The values of the longitudinal and lateral correlation functions, Ψ_{Ω} $(\xi,0,0)$ and Ψ $(0,\eta,0)$, are shown in Figures (6a) and (6b), respectively. The longitudinal space-time correlation function, Ψ_{Ω} $(\xi,0,\tau)$ is given by Figure (7) and the r.m.s. pressure is plotted versus the Strouhal number, $\omega\delta/U_0$ in Figure (8).

Bull's results showed that the spectral density expressed in terms of wall shear stress increases with Reynolds number although at a considerably smaller rate than suggested by the r.m.s. pressure fluctuations measurements. Also his measurements proved that the longitudinal velocity disturbance at a particular distance from the wall is convected at the speed of the local mean flow.

On the other hand, more research work by Bull [37] has been carried out to predict the wall-pressure field, i.e. the statistical quantities such as the r.m.s. pressure, frequency power spectrum, space-time correlations and space-time correlation measurements in both broad and narrow frequency bands. His experiments were made at Mach Number of 0.3 and 0.5 with covered Reynolds Numbers of 10^5.

The main conclusions of Bull measurements were that the wall-pressure field structure is produced by contribution from pressure sources in the boundary-layer with a wide range of convection velocities and comprises two families of convected wave number components. One family of high wave number components is associated with turbulent motion in the constant stress layer. The second family comprises components of wave length greater than about twice the boundary-layer thickness, which lose coherence as a group of wave length and are associated with large scale eddy motion in the boundary-layer outside the constant stress layer. Bull discussed the pressure field in terms of these two-wave number families.

3.2   Wall-pressure fluctuations of body of revolution

The problem of predicting the wall-pressure fluctuations of a
body of revolution was studied recently by Lyamshev et al. [40].
The influence of fluid section from turbulent boundary-layer on the
spectral and correlative properties of the wall-pressure fluctuations
has been conducted experimentally using a model with a chord length
of 500 mm and span of 120 mm.

The model was set up in the rectangular working section of the
tunnel at zero angle of attack. "Identical pressure fluctuations sen-
sors whose sensitive surface has a diameter of 1.5 mm were mounted
flush with the lateral surface of the model at various distances from
the bow tip". The spectral and correlative properties were measured
in the frequency range from 0.1 to 10 KHz and free stream velocity
varied from 3 to 18 m/sec, with Reynolds Number up to 10^7. The spec-
tral and correlation analysis data obtained by Iyamshev were carried
out in third octave frequency bands.

Lyamshev concluded that an increase in the relative rate of the
distributed fluid suction from a well developed turbulent boundary-
layer causes a decrease in the longitudinal spatial correlation and
a decrease in the spectral power density of the wall-pressure fluc-
tuations in the low frequency range. On the other hand these effects
are increased in the high frequency part of the spectrum due to the noise
emission and the amount of increase depends on the suction rate and
the relative intensities of the noise and pseudosonic components of

the signals. Also he deduced that the boundary-layer suction does not affect the correlation properties of the wall-pressure fluctuations in the high frequency part of the spectrum.

Another interesting experimental investigation of the correlative characteristics of turbulent wall-pressure fluctuations has been performed by Kodykav $\begin{bmatrix} 41 \end{bmatrix}$. His measurements were conducted on the surface of a model of half body of revolution of elementry configuration, subjected to flow velocity ranging from 8 to 24 m/sec. The pressure pickups with a sensing surface of 1.5 mm in diameter were mounted flush with model surface. The spacings between pickups were fixed at 4.2, 10, 29.2 mm. The correlation analysis was carried out in 1/3 octave bands over frequency range from 150 to 3,000 Hz. The fluctuations noise spectrum was recorded concurrently over a wide range of frequencies.

It was established throughout Kodykav experiments that the correlation characteristics of large-scale turbulent wall-pressure fluctuations for which the hydrodynamic wave length is greater than the boundary-layer thickness are subjected to different laws than those obeyed by small-scale fluctuations. Kodykav concluded that the boundary-layer thickness is a factor governing on the one hand, the maximum vortex dimension in the turbulent boundary-layer and on the other hand, the statistical properties (the correlation radius in particular) of the large-scale inhomogenities formed by those vortices. Finally he pointed out that his results were particularly important when it comes to take into account the influence of the pressure pickup dimensions on the recording of turbulent wall fluctuations.

Moreover, a research work studying the statistical properties of wall-pressure fluctuations on a body of revolution in water medium with Reynolds Number of 3.94 X 10^7 to 1.18 X 10^8 was carried out by Backewell [42] , using a flush-mounted hydrophones as pickup transducers. His measurements were conducted not only for stream-wise and lateral hydrophone separations but also for hydrophone separations oriented at angles of 26.5^0 and 45^0 to the flow axis.

Backewell, presented the nondimensionalized spectral and correlation data which are in a good agreement with zero and nearly zero pressure gradient obtained for a flat plates and in fully developed pipe flow, respectively. One of the main con-clusions of Backewell data is that the magnitude of the general cross spectral density is approximately equal to the product of the magnitude of longitudinal and lateral cross-spectral densities. Backewell's experimental results confirm Corco's assumption at this fact.

3.3   Wall-pressure fluctuations of pipe flow

3.3.1   Air flow

Measurements of wall-pressure fluctuations were performed by W.W. Willmarth [43] , using test section of 4" brass pipe, with barium titanate pressure transducers as pickups in air flow. The spectrum of the wall-pressure is presented in nondimensional form. Willmarth drew three important conclusions from his investigations:

a) the ratio of r.m.s. wall-pressure fluctuations to free stream

dynamic pressure, $\overline{(p^2)}^{\frac{1}{2}} / q_\infty$, is not dependent on Mach or Reynolds

Number and approaches the value 0.006 and d/δ approaches zero

(where q_∞ is the free-stream pressure, d is the diameter of the

pressure transducer, and δ is the boundary-layer thickness);

b) the mean square pressure fluctuations, $\overline{p_\Omega^2}$ (t), may be thrown

into a dimensionless form as shown in Fig. 9, and c) the random

pressure fluctuations are convected at speed of the order

$U_c = 0.82\ U_\infty$ (where U_c is the convection velocity and U_∞ is the

centerline velocity).

Another investigation by Willmarth and Yang [51] predicts the

measurements of turbulent wall-pressure fluctuations on the outer

surface of a 3" diameter cylinder aligned with the flow. At a

point approximately 24 ft down-stream of the origin in an air stream

of 145 ft/sec. The boundary-layer thickness was 2.78" and the

Reynolds Number based on the momentum thickness was 2.62×10^4. A

0.06" diameter lead zirconate-titanate disk transducers were mounted

flush with the wall.

Willmarth and Yang found that the longitudinal and transverse

scales of the pressure correlations are approximately equal and in a

plane boundary-layer the transverse scale is larger than longitudinal

scale within one-half or less than the longitudinal scale in the pla-

ne boundary-layer. He also concluded that the effect of the trans-

verse curvature of the wall is an overall reduction in size of pres-

sure producing eddies, and the reduction in transverse scale of the larger

eddies is greater than that of the small eddies. Generally he concluded

that the smaller eddies decay more rapidly and produce greater spec-
tral densities at high frequencies due to the undamped convective
speed.

In 1962, Backewell et al. [44,46], investigated the statistical
properties of the wall-pressure field induced by turbulent air flow
at the wall of thin cylindrical shell over broad frequency bands and
in octave frequency bands for limited range of Reynolds Numbers
(10^5 to 3 X 10^5). They measured and derived expressions for the axial,
Ψ_Ω (ξ, 0, 0), and circumferential, Ψ_Ω (0, η, 0), correlation func-
tions as shown in Figures 10 and 11, respectively. Bakewell [44] found
that his experimental points defined the following approximate expres-
sions for the spatial correlations:

$$\Psi_\Omega\ (\xi,0,0) = e^{-b|S_\xi|} \cos a\ S_\xi, \tag{14}$$

$$\Psi_\Omega\ (0,\ \eta,\ 0) = (1 + cS_\eta^2)^{-1}\left[2 - e^{-dS_\eta^2} \right]^{-1}, \tag{15}$$

where $S_\xi = \xi\Omega/U_c$ and $S_\eta = \eta\Omega/U_\infty$ are the axial and circumferential
Strouhal numbers, and a,b,c,d are constants to be specified; U_c and
U_∞ are, respectively, the convection and centerline velocities.

As shown in reference [44], the effects of Reynold number on the
spatial correlations are small and may be neglected. The values of
a,b,c, and d to be used in equations (14) and (15) are as follows:

a = 8.7266, b = 1.0 for $S_\xi = \xi\Omega/U_\infty$,

c = 20 , d = 100 for $S_\eta = \eta\Omega/U_\infty$

Bakewell also obtained measurements of the mean $\overline{\text{square pressure}}$ per unit bandwith (i.e. the power spectral density), $\overline{p_\Omega^2}$ (t), which are reproduced in Fig. 12 plotted against Strouhal number $2r\Omega/U_\infty$. For the purpose of their analysis Lakis and $\underline{\text{Paidoussis}}$ [12] derived an expression for the curve of best fit of $\overline{p_\Omega^2}$ (t):

$$\overline{p_\Omega^2}\ (t) = 2k_2\ \rho_F^2\ rU_\infty^3\ e^{-2k_1 r\Omega/U_\infty}\ , \tag{16}$$

where $k_1 = 0.25$, $k_2 = 2 \times 10^{-6}$ and ρ_F is the density of the fluid.

The ratio of the broad band convection velocity to the center-line velocity U_c/U_∞ has been determined by Bakewell et al. and plotted against the Reynold numbers. This ratio has the value of approximately 0.7 and appears to be independent of Reynolds number. It is lower than the 0.80 obtained by Willmarth [43] and other investigators. Finally the ratio of the r.m.s. pressure to the dynamic pressure, $\overline{p_\Omega^2}\ (t)^{\frac{1}{2}} \Big/ \frac{1}{2}\ \rho_F\ U_\infty^2$, is approximately 0.006 for different Reynolds number. This value is within the range of values reported by other investigators [43,35,53].

3.3.2 Water flow

It may be expected that the spatial correlation given by equations (14), (16) and determined by Bakewell et al. of air flow in pipe would be approximately the same for different fluids at the same Strouhal number, at least for sufficiently high Reynolds number. This was supported by Clinch's measurements of the statistical properties of wall-pressure field generated by the passage of fully developed turbulent

water flow in smooth pipe [49]. He applied test section of 6 inches diameter connected to a water loop facility capable of producing Reynolds number of 2 X 10^6. The measurements of wall-pressure fluctuations were recorded by flush mounted miniature pressure transducers. The statistical properties of the wall-pressure field determined by Clinch included the power spectral density, space-time correlations, and convection velocities performed in both broad and narrow frequency bands.

Rattayya and Junger [50] reviewed recent data on the correlation function describing the random pressures in the turbulent boundary-layer and they predicted the response of a pipe using Bakewell's correlation functions [44,46].

Carey et al. [49] designed and constructed at the U.S. Navy Underwater Sound Laboratory an acoustic Turbulent Water-Flow Tunnel using a clear-plastic-pipe test section of 3.5 in i.d. through which water is pumped at centerline velocities ranging from 9 to 48 knots. Their measurements of the ratio of convection velocity to centerline velocity, U_c/U_∞, range from 0.86 to 0.61 using flush-mounted hydrophones at several longitudinal spacings. They also found that the maximum space-time is in good agreement whith other investigators [46,53]. The corrected data for hydrophone size showed also that the spectral curve is similar to those reported for turbulent air flow and falling bodies in water [42].

3.4   Influence of pickups shape and orientation on wall-pressure fluctuations measurements

A recent theory of transducers resolution of flow noise (wall-pressure fluctuations under turbulent boundary-layer) developed by Kirby [52] shows that the resolution depends only on the face area and the maximum face widths of the transducer normal and parallel to the flow direction. All Kirby results are valid only for transducers with dimensions within the range of 3 to 100 of, $\Omega A^{\frac{1}{2}}/U_\infty$, (where Ω is frequency, A is the transducer area and U_∞ is the centerline velocity). The effect of transducer free width parallel to the flow is small and negligible.

Kirby found also that "for transducers of given area the wall-pressure fluctuations level resolved is nearly proportional to the face width normal to the flow, so that slender transducers should have their long axis parallel to the flow to increase the signal-to-noise ratio". He also showed that his theory agrees with experimental data on circular, square and fish shaped transducers within experimental accuracy.

Meanwhile, the response of a flush-mounted transducers to the pressure field in a turbulent boundary-layer is known to depend upon the spatial and temporal characteristics of the transducers. An experimental study of this dependence has been conducted by Geib [39].

The frequency spectral density of the pressure fluctuations on the boundary beneath a turbulent boundary-layer was measured with various transducers radii. The wind tunnel employed in Geib experiments is a closde circuit subsonic flow with 15 X 18 inches of cross-section and using a ½ inch condenser microphone as pickup.

The results obtained by Geib present typical frequency spectral density in nondimensional form; a market decrease in the spectral density values are evident as the transducer radius increased.

In addition, Lyamshev [59] performed pressure fluctuations measurements by applying means of pressure pickups of the piston type whose membrane is fixed flush with a surface of the body. The hydrodynamic pressure fluctuations spectrum were performed using various dimensions of pickups.

Lyamshes results showed that the geometric dimensions and shape of the pickups may exert a substantial influence on the measured results of the pressure fluctuation spectrum.

Finally, a detailed design of an assembly of a miniature transducers for wall-pressure fluctuation measurements in turbulent boundary-layer flows was described by Clinch [47]. His calibration of this transducer indicated that its sensivity is near -130dB-re- 1v/μBar at sound pressure levels varying from 135 to 160dB.

3.5 Wall-pressure fluctuations structures

A discussion of the statistical properties of pressure field at the wall of a turbulent attached shear flows has been performed by Corcos [45] , explaining the important limitations imposed by the imperfect space resolution of contemporary transducers. He also showed that the measurements of the longitudinal cross correlation densities lead to similarity variables for the space-time covariance of the pressure and for the corresponding spectra. He also explained the existance of those similarities, due to the dispersion of the sources of pressure by the mean velocity gradient. Corcos tried to interpret analytically some of these pressure measurements by pointing out that the lateral cross-spectral densities lead approximately to similarity variables.

However, Corcos carried out computations based directly upon the pressure-velocity correlation measurements by Wooldrige and Willmarth for flat plate and Backewell [44] for pipe flow. The interaction of the mean strain rate with normal velocity fluctuations being in effect limited to a region very near to the wall, supplies a dominant contribution only at high frequencies. He illustrated also that the downstream convection speed and convective memory

are smaller than those of the observed wall-pressure.

Corcos emphasis also that "the inner part of the law of the wall region seems to be substantially free of pressure sources and within that region (a) the pressure can be given in terms of its boundary value and (b) the local velocity field is dependent upon but unable to affect appreciably the turbulent pressure".

Moreover, it is well known, that the finite size of a transducer-sensing element limits its space resolution of a pressure field associated with a local turbulent flow. Such pressure fields are translated at a speed comparable to the characteristic velocity of the flow. Consequently a lack of space resolution of the face of the transducers used caused an apparent inability to solve the problem which is examined by Corcos $\begin{bmatrix} 53 \end{bmatrix}$.

He applied numerical results which indicate that the attenuation of frequency spectral density and of the cross-spectral density caused by the finite size of the transducers is generally more severe than previous computation had suggested. Mainly because the lateral correlation of pressure is highly frequency dependent, and a typical turbulent pressure wave component being inclined to the stream direction at roughly 45 degrees. An asymptotic formulas for the attenuation of large transducers were given by Corcos which yield estimation of the degree to which a flush-mounted sensor

reciever immersed in a boundary-layer is able to reject the background noise provided by turbulent pressure fluctuations.

Recently, Mulhearn [54] calculated the pressure and pressure-velocity space correlations using rapid distortion theory for turbulence in a uniform shear flow. He found that the pressure fluctuations remain correlated over a significantly greater distances than the velocity fluctuations. Applying these predictions as a model for turbulence in free turbulent shear flows, he proved that the predicted scale of the pressure fluctuations is larger than the flow width. It is proposed that the wall-pressure fluctuations remain correlated right across free shear flows.

Mulhearn compared the prediction from the rapid distortion theory with various experimental measurements for pipe flow, flat plate and panels with different situations in which reasonable qualitative agreement is achieved.

Finally one of the interested investigation in the wall-pressure fluctuation field has been performed by Schloemer [38]. He studied the normalized longitudinal and lateral cross spectral density and the convection velocity ratio as a function of longitudinal separation and frequency of wall-pressure fluctuations. Comparison with the work of other investigators as shown in Fig. 13, is excellent. He measured those parameters with a small flush-mounted transducer (lead zirconate titanate ceramic disk of 0.06 inch in diameter).

The facility was simply flat aluminum plate instaled in 1 X 12
feet test section of a tunnel provided with areafoil section for
the sake of creating pressure gradients. These measurements are
accomplished in both mild adverse and mild favorable pressure
gradients in a law turbulence subsonic flow.

The effect of an adverse pressure gradient on the nondimen-
sionalized spectral density was an increase in the flow frequency
content without influencing the high-frequency portion. Schloemer
observed a sharp decrease in the high frequency portion for the
favorable pressure gradient. At similar nondimensional longitudinal
separations and frequencies, the convection velocity ratio was
higher in the favorable and lower in the adverse pressure gradients.
He also noticed that the longitudinal decay of a particular eddy
is more rapid in the adverse and slower in the favorable pressure
gradients, and no differences were found in the lateral cross spec-
tral density for the different pressure gradient.

4.   CONCLUSION

In this paper we have presented a review of the different inves-
tigations of cylindrical shells response and the statistical properties
of the wall-pressure fluctuations. To this end the techniques used to
obtain the response of cylindrical shells subjected to internal pres-
sure, acoustic, random and turbulent boundary-layer excitations are
reviewed in details. Of these the most versatile have proved to be

Rayleigh-Ritz methods [15] and the hybrid classical/finite-element

methods [12,33]. The later has added advantages in terms of ease

of formulation, and because numerical convergence is not as sensi-

tive to particular set of boundary conditions as is the case with

the Rayleigh-Ritz method [15]. In Lakis and Paidoussis method [33],

the thin shell equations are used in full for the determination of

the displacement functions instead of the more usual polynomial

displacement functions. The random pressure forces are lumped at

the nodes of the finite elements and the mean square value of the

displacements of the shell are obtained for an arbitrary pressure

field and for a boundary-layer pressure fluctuations.

There are several reasons for undertaking the development of

this hybrid classical/finite-element theory [12]. First, existing

theories have been generally developed for special cases; the need

is evident for a theory which can be used for the dynamical analysis

of any kind of circular cylindrical shell which is geometrically

axially symmetric. A practical case in point is concerned with the

prediction of the natural frequencies of the outer containment

shell and of the inner shroud of shell-and-tube heat exchangers,

where both ring stiffeners and several thickness and material dis-

continuities are present. A second reason is that ordinary finite-

element theories cannot easily be used to analyse liquid-filled

cylindrical shells. On the other hand, the theory of Lakis and

Paidoussis $\begin{bmatrix}12\end{bmatrix}$, because of its usage of classical theory for the displacement functions, can easily be adopted to take the hydrodynamic effects into account. Finally, again because of the use of classical theory, we can obtain the high as well as the low frequencies with high accuracy. This is normally of little interest for free vibration analysis, but is of considerable importance in the determination of the response of such shells to random pressure fields, such as pressure fields generated by internal or external flow. Accordingly, this theory $\begin{bmatrix}12\end{bmatrix}$ is much more precise than the usual finite-element methods, but suffers from lack of versatility; for instance, it cannot be used to analyse anything other than circular cylindrical shells, or right-circular conical shells.

Our review of the wall-pressure fluctuations covered experimental investigations on panel, body of revolution and cylindrical shell subjected to a fully developed boundary-layer arising from an internal flow. The transducers size, shape and orientation were also discussed. The following conclusions were made in the special case of the boundary-layer excitations.

(i) The non-dimensional power spectral density of the wall-pressure fluctuations may be expressed in terms of Strouhal number.

(ii) For a given pipe diameter, the frequencies of the wall-pressure fluctuations show scaling with flow speed.

(iii) The averaging effects of a finite size hydrophone on the wall spectra may be eliminated by the use of Corcos' hydrophone size corrections $\lfloor 53 \rfloor$.

(iv) The overall intensity of the pressure fluctuations is essentially constant and not dependent on Mach or Reynolds numbers.

(v) The ratio of convection velocity, which represents the speed at which a disturbance is transported downstream, to centerline velocity (U_c/U_∞) range from 0.81 to 0.6, Fig. 14

(vi) The validity of the separability of the spatial cross-correlation function, Ψ_Ω (ξ, η, 0), into a product of circumferential correlation function, Ψ_Ω (0, η, 0), and longitudinal correlation function, Ψ_Ω (ξ, 0, 0), as suggested by Corcos, appears to be verified well by Bakewell $\lfloor 42 \rfloor$ within the limits of experimental accuracy.

(vii) The circumferential and longitudinal correlation functions predicted for subsonic water pipe flow $\lfloor 48 \rfloor$, show similar characteristics to those predicted for air flow in pipe $\lfloor 46 \rfloor$.

(viii) The statistical properties, p_Ω^2 (t), $\Psi_{p\Omega}$ (ξ, 0, 0) and Ψ_Ω (0, η, 0), of the wall-pressure fluctuations in a turbulent boundary-layer on a body of revolution (near zero-pressure gradient) show a good agreement with data obtained in flat plate boundary-layer and in pipe flows, Figures (15 and 16)

An experimental investigation to predict the statistical properties in thin-walled cylindrical shell subjected to internal turbulent

two-phase flow is in progress. A continuously operating air-water flow facility capable of producing Reynolds number of 1.5×10^6 is designed for this investigation. A comparison will be made, by using the theory of $\left[12\right]$, between the predicted response of the thin-walled shell with that measured experimentally over a wide range of flow speeds, mixture ratio, and exciting frequencies. A more general study, however, would be more detailed examination of the effect of fluid cavitation on the response.

Acknowledgments

REFERENCES

1. LOVE, A.E.H. "A Treatise on the Mathematical Theory of Elasticity", 1944, A $\underline{\text{th}}$ edition, Chap. 24, (Dover, New-York).

2. FLUGGE, W. "Stresses in Shells", 1960, Springer-Verlag-Berlin.

3. SANDERS, J.L. "An Improved First Approximation Theory for Thin Shells", NASA-TR, R24, 1959.

4. COTTIS, M.G. and JASONIDES, J.G. "The Response of a Finite Thin Cylindrical Shell to Random Pressure Field". Proceeding of the second international Conference Dayton, Ohio, April 29 to May 1st, 1964 (Acoustic Fatigue in Aerospace Structures).

5. COOPER, P.A. "Vibration and Buckling of Prestressed Shells of Revolution", NASA-TN, D-3831, 1967.

6. CLINCH, J.M. "Prediction and Measurements of the Vibrations Induced in Thin-Walled Pipes by the Passage of Internal Turbulent Water Flow". J. Sound and Vibration 12, 429-451, 1970.

7. CLINCH, J.M. "Study of Vibrations Induced in Thin-Walled Pipes Under Varying Flow Conditions". Contract No. NAS8-20325, 1967.

8. CORCOS, G.M. and LIEPMANN, H.W. "On the Contribution of Turbulent Boundary-Layer to the Noise Inside a Fuselage". NASA T.M. 1420, 1956.

9. NASH, W.A. and KAHEMATSU, H. "Random Vibrations of Shallow
    Shells". Symposium on shells and climatic influences, Cal-
    gary 1972, Report for session on special topics.

10. SEWALL, J.L. and NAUMANN, E.C. "An Experimental and Analyti-
    cal Vibration Sutdy of Thin Cylindrical Shells With and Without
    Longitudinal Stiffeners. NASA-TN-D-4075, 1968.

11. COHEN, G.A. "Computer Analysis of Asymmetric Free Vibrations
    of Ring-Stiffened Orthotropic Shells of Revolution". AIAA, J.,
    1965, $\underline{3}$, 2305.

12. LAKIS, A.A. and PAIDOUSSIS, M.P. "Prediction of the Response
    of a Cylindrical Shell to Arbitrary or Boundary-Layer Induced
    Random Pressure Field. J. Sound and Vibration, 1972, Vol. 25,
    1-27.

13. MAGRAB, E.B. and BURROUGHS, C. "Forced Harmonic and Random
    Vibrations of Concentric Cylindrical Shells Immersed in A-
    coustic Fluids". J. Acoust. Suct. of Am., Vol. 52, #3, 1972.

14. NASSER, S.N. "On the Response of Shallow Thin Shells to Random
    Excitation". AIAA, J., Vol. 6, #7, p. 1327, 1968.

15. DYM, C.L. "Vibrations of Pressurized Orthotropic Cylindrical
    Membranes". AIAA, J., (8), #4, 1970.

16. THOMPSON, J.J. and NOLY, Z.J. "Random Pressure-Induced Vibration
    of Pinended Cylindrical Rods and Tubes". Nuclear Engineering and
    Design 33, 370-380, 1975.

17. HWANG, C. and PI, W.S. "Random Acoustic Response of a Cylindrical Shell". AIAA, J. (7), #12, 2204, 1970.

18. HAMADA, M. and MASE, M. "Free Vibration Problem of Pressurized Axisymmetrical Shells". JSME, (17), #12, 1974.

19. VAFAKAS, W.P., ROMANO, F. and KEMPNER, J. "Clamped Short Oval Cylindrical Shells Under Hydrostatic Pressure". J. Aerospace Science, 1962, p. 1347.

20. FUNG, T.C., SECHLER, E.E. and KAPLAN, A. "On the Vibration of Thin Cylindrical Shells Under Internal Pressure". J. Aeronautical Science, Sept. 1957.

21. KANA, D.D. "Response of a Cylindrical Shell to Random Acoustic Excitation". AIAA, J. Vol. 9, #3, 1971.

22. COTTIS,M.G. "On the Dynamic Response of an Orthotropic Finite Cylindrical Shell to an Arbitrary Pressure Field". J. Sound and Vibration 7 (1), 31-38, 1968.

23. PING, A. and WANG, L. "A Note on the Random Response of a Thin Cylindrical Shell". J. Sound and Vibration 12, (4), 393-396, 1970.

24. LAKIS, A.A. and DORE, R. "Dynamic Analysis of Anisotropic Thin Cylindrical Shells Subjected to Boundary-Layer Induced Random Pressure Fields". Ecole Polytechnique de Montréal, Report 74-R-27, 1974.

25. WEYERS, P.F.R. "Vibration and Near Field Sound of Thin-
     Walled Cylindrical Caused by Internal Flow". NASA-TN-D430,
     1959.

26. KHOSROVANI, H., COHEN, R. and CHANAUD, R.C. "Response of a
     Thin-Walled Cylindrical Duct to Internal Air Flow". J.
     Acoustic Socit. Am. (50), #1, 1971.

27. POWELL, A. "Vibrations Excited by Random Pressure Field".
     J. Acoust. Scoit. Am., 30, 1130-1135, 1958.

28. LAKIS, A.A. and PAIDOUSSIS, M.P. "Dynamic Analysis of Axially
     Non-Uniform Thin Shells". I. Matrix Formulation. J. Mech.
     Engg. Sci (14), 49-71, 1972.

29. LAKIS, A.A. "Free Vibration and Response to Random Pressure
     Field on Non-Uniform Cylindrical Shells". Ph.D. Thesis,
     McGill University, 1971.

30. BUDIANSKY, B. and SANDERS, J.L. "On the "Best" First Order
     Linear Shell Theory". Progress in Applied Mechanics, 1963,
     p. 129.

31. AIENKIEWICZ, O.C. and CHENNY, Y.K. "The Finite Element Method
     in Structural and Continuum Mechanics, New-York, McGraw-Hill, 1968.

32. MERCER, C.A. and HAMMOND, J.K. "On the Representation of Conti-
     nuous Random Pressure Fields at a Finite Set of Points". J.
     Sound and Vibration, (7), 49-61, 1968.

33. LAKIS, A.A. and PAIDOUSSIS, M.P. "Dynamic Analysis of Axially Non-Uniform Thin Cylindrical Shells". J. Mech. Engg. Sci. (14), 49-71, 1972.

34. TOWNSEND, A.A. "Entrainment and the Structure of Turbulent Flow". J. Fluid Mech. (41), 13, 1970.

35. TACK, D.H., SMITH, M.W. and LAMBERT, R.F. "Wall Pressure Correlation in Turbulent Air Flow". J. Acoust. Socit. Am. (33), #14, 1961.

36. BULL, M.K. "Properties of the Fluctuating Wall-Pressure Field of a Turbulent Boundary-Layer". AGARD, Rept. No. 455, 1963.

37. BULL, M.K. "Wall-Pressure Fluctuations Associated with Turbulent Boundary-Layer". J. Fluid Mech., Vol. 42, #1, 1967.

38. SCHLOEMER, H.H. "Effects of Pressure Gradients on Turbulent Boundary-Layer Wall-Pressure Fluctuations. J. Acoust. Socit. Am., Vol. 421, #1, 1967.

39. GEIB, F.E. Jr. "Measurements on the Effect of Transducer Size on the Resolution of Boundary-Layer Pressure Fluctuation. T. Acoust. Scoit. Am., vol. 46, #1, 1969.

40. LYAMSHEV, L.M., PUZINO, M.G. and SALOSSINA, S.A. "Characteristics of Pressure Fluctuations in Distributed Section of a Turbulent Boundary-Layer". Sov. Phys. Acoust., Vol. 20, #5, 1975.

41. KODYKAV, J.F. "Experimental Sutdy of the Longitudinal Space
     Time Correlation Function of Turbulent Wall-Pressure Fluc-
     tuations". Sov. Phys. Acoust., Vol. 17, #1, 1971.

42. BACKEWELL, H.P. Jr. "Turbulent Wall-Pressure Fluctuations on
     a Body of Revolution". J. Acoust. Socit. Am., Vol. 43, #6,
     p. 1358, 1968.

43. WILLMARTH, W.W. "Space-Time Correlation and Spectra of Wall-
     Pressure in a Turbulent Boundary-Layer". NASA M. 3-17 59 W,
     1959.

44. BACKEWELL, H.P. Jr. "Narrow-Band Investigations of the Longi-
     tudinal Space-Time Correlation Functions in Turbulent Air Flow".
     J. Acoust. Socit. Am., Vol. 36, #1, 1964.

45. CORCOS, G.M. "The Structure of the Turbulent Pressure Field
     in Boundary-Layer". J. Fluid Mech., Vol. 18, p. 253, 1963.

46. BACKEWELL, H.P. Jr. "Wall-Pressure Correlation in Turbulent
     Pipe Flow". U.S. Navy Underwater Sound Laboratory, New Lon-
     don, Connecticut, U.S.L. Report No. 559, 1962.

47. CLINCH, J.M. "Miniature Transducers Assembly for Measuring
     the Properties of the Wall-Pressure Field in Turbulent Flows".
     J. Acoust. Socit. Am., Vol. 40, #1, 1966.

48. CLINCH, J.M. "Measurements of the Wall-Pressure Field at the
     Surface of a Smooth-Walled Pipe Containing Turbulent Water
     Flow". J. Sound and Vibration, 9, (3), 398, 1969.

49.   CAREY, G.F. "Acoustic Turbulent Water, Flow Tunnel". J.
        Acoust. Socit. Am., Vol. 41, #2, 373, 1967.

50.   RATTAYYA, J.V. and JUNGER, M.C. "Flow Excitation of Cylin-
        drical Shells and Associated Coincidences Effects". J.
        Acoust. Socit. Am., Vol. 36, #6, 1964.

51.   WILLMARTH, W.W. and YANG, C.S. "Wall-Pressure Fluctuations
        Beneath Turbulent Boundary-Layer on a Flat Plate and a Cy-
        linder". J. Fluid Mech., Vol. 41, part 1, 47, 1970.

52.   KIRBY, G.J. "The Effect of Transducer Size, Shape and Orien-
        tation the Resolution of Boundary-Layer Pressure Fluctuations
        at a Rigid Wall". J. Sound and Vibration, 10, (30' 361, 1969.

53.   CORCOS, G.M. "Resolution of Pressure in Turbulence". J. Acoust.
        Socit. Am., Vol. 35, #2, 1963.

54.   MULHEARN, P.J. "On the Structure of Pressure Fluctuations in
        Turbulent Shear Flow". J. Fluid Mechanics, Vol. 71, part 4, 801,
        1975.

55.   LYAMSHEV, L.M. and SALOSINA, S.A. "Influence of the Pickup Di-
        mension Measurements of the Spectrum Wall-Pressure Fluctuations
        in a Boundary-Layer". Sov. Phys. Acoust., Vol. 12, #2, 1966.

56.   TOWNSEND, A.A. "The Structure of Turbulent Shear Flow".
        Cambridge University Press, 1956.

57. KRAICHNAN, R.H. "Pressure Fluctuations in Turbulent Flow Over a Flat Plate". J. Acoustic Soc. Am. 28, 1956, p. 378.

58. LILLEY, G.M. and HODGSON, T.H. "On Surface Pressure Fluctuations in Turbulent Boundary-Layer". Agard Report 276, 1960.

59. LILLEY, G.M. "Wall-Pressure Fluctuations Under Turbulent Boundary-Layers at Subsonic and Supersonic Speeds". Agard Report 454, 1963.

60. DEISSLER, R.G. "Pressure Fluctuations in a Weak Turbulent Field with a Uniform Transverse Velocity Gradient". Phys. Fluids, 5, 1124, 1962.

61. LAKIS, A.A. "Effects of Fluid Pressures on the Vibration Characteristics of Cylindrical Vessels". Proceeding of the Second International Conference on Pressure Surges. BHRA Fluid Engineering, Cranfield, Bedford, England, 1976.

NOTATIONS

a, b, c, d   Constants defined in equation (14, 15).

A, B, C, D   Constants defined in equation (4).

$f_{rn}(x,t)$, $f_{cn}(x,t)$ Instantaneous radial and circumferential forces per unit length.

$\overline{f\Omega \; f'\Omega}$ Mean of the force f per unit bond width.

J   number of constraints imposed.

l Length of finite element.

l_e Co-ordinate of node e in the x - direction.

l'_e, l''_e Co-ordinates of the area S_e, surrounding the node e, with respect to the origin in the x - direction.

L   Total length of shell.

m   Axial half wavenumber.

M_r Moment acting at node as shown in (Fig. 3).

n   Circumferential wavenumber.

N   Number of finite elements.

$P(x, \phi, t)$ Instanteneous pressure on the surface.

$\overline{P^2}(x, \phi, t)$ Mean square of the pressure per unit band width of a homogeneous pressure field.

q_∞ Free - stream pressure.

r Mean radius of shell.

$Re \left[\ \right]$ Real part of $\left[\ \right]$.

S_ξ, S_η Axial and circumferential Strouhal number.

S_e Area surrounding the node e (Fig. 3).

t Wall-thickness of the shell.

U, V, W Axial, circumferential and radial displacement.

U_∞, U_0, U Centerline velocity.

U_c Convective velocity.

$\overline{U}$ Mean flow velocity.

$\overline{U}_i$ Dimensionless flow velocity.

u_n, v_n, w_n Amplitudes of U, V, W associated with n^{th} circumferential wavenumber.

$W_f (x_i, x_j, \Omega)$ Cross-correlation spectral density function of the force field.

x Axial coordinate.

$y_g \ (x_g, \ \phi, \ t)$	Mean square displacement of Un, Vn, Wn or $\dfrac{dwn}{dx}$ at node for which $x = x_g$
ξ_r	Generalized damping factor.
η	Equal to $\left\| r \ (\phi_i - \phi_j) \right\|$.
ν	Poisson's ratio.
ξ	Equal to $\left\| x_i - x_j \right\|$.
ρ	Density of material of shell.
ρ_f	Fluid density.
τ	Time delay.
ϕ	Circumferential coordinate.
$\Psi_{p\Omega} \ (\xi, \ 0, \ 0)$ $\Psi_{p\Omega} \ (0, \ \eta, \ 0)$	Axial and circumferential correlation functions of the fluctuating pressure per unit band width with centre frequency Ω.
ω	Natural frequency Hz.
Ω	Excitation circular frequency (rad./sec.).
ζ	Time delay.
θ_1	Time rate of decay of coherence.
δ^*	Boundary layer thickness
$F \ (x, \ \phi, \ t)$	Vector of external forces.

$\begin{bmatrix} k \end{bmatrix}$ Stiffness matrix for one element.

$\begin{bmatrix} K \end{bmatrix}$ Stiffness matrix for the whole structure.

$\begin{bmatrix} m \end{bmatrix}$ Mass matrix for one finite element.

$\begin{bmatrix} M \end{bmatrix}$ Mass matrix for the whole shell.

M Generalized mass matrix (for the whole shell).

$\{y\}$ Displacement vector.

$\{\delta_i\}$, $\{\delta_j\}$ Nodal displacements vectors, at nodes i and j respectively.

$\begin{bmatrix} \Phi \end{bmatrix}$ Nodal matrix of the system.

$\{\Phi_r\}$ r^{th} eigen vector of the system.
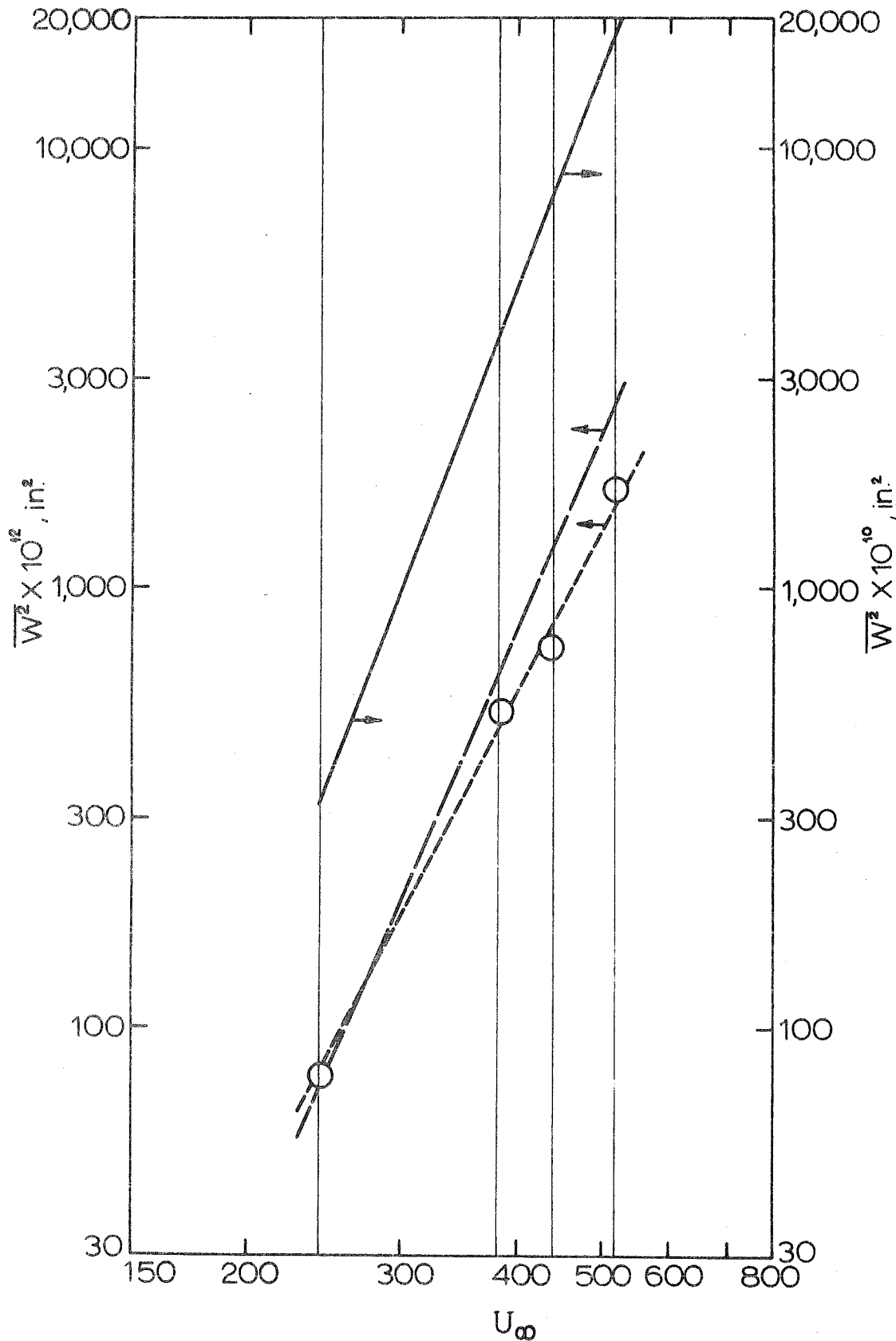
FIGURE 1 The mean square response of the radial displacement
of a shell first studied by Clinch, as a function of
the centerline velocity. -0--0- Clinch's experimental
results for high-frequency response; — — —   theoret-
ical results obtained by Lakis [12]   (with n = 2 to
n = 6) for high-frequency response (93 - 1,000 Hz):
——— 'total' response obtained by Lakis [12]   (with
n = 2 to n = 6).
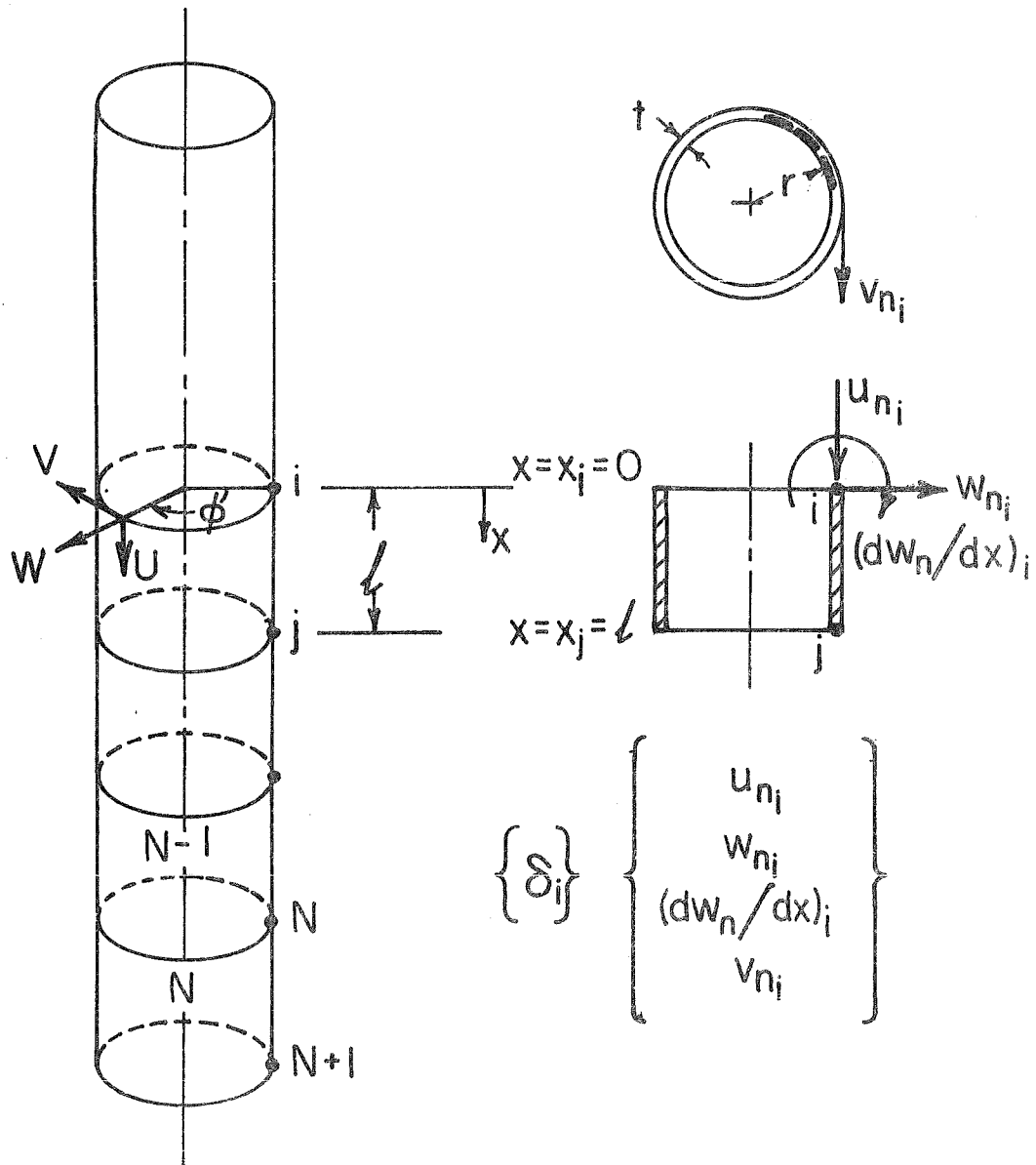
FIGURE 2 Definitions of the finite element used

and of the displacement vector $\underset{\sim}{\delta}_i$.
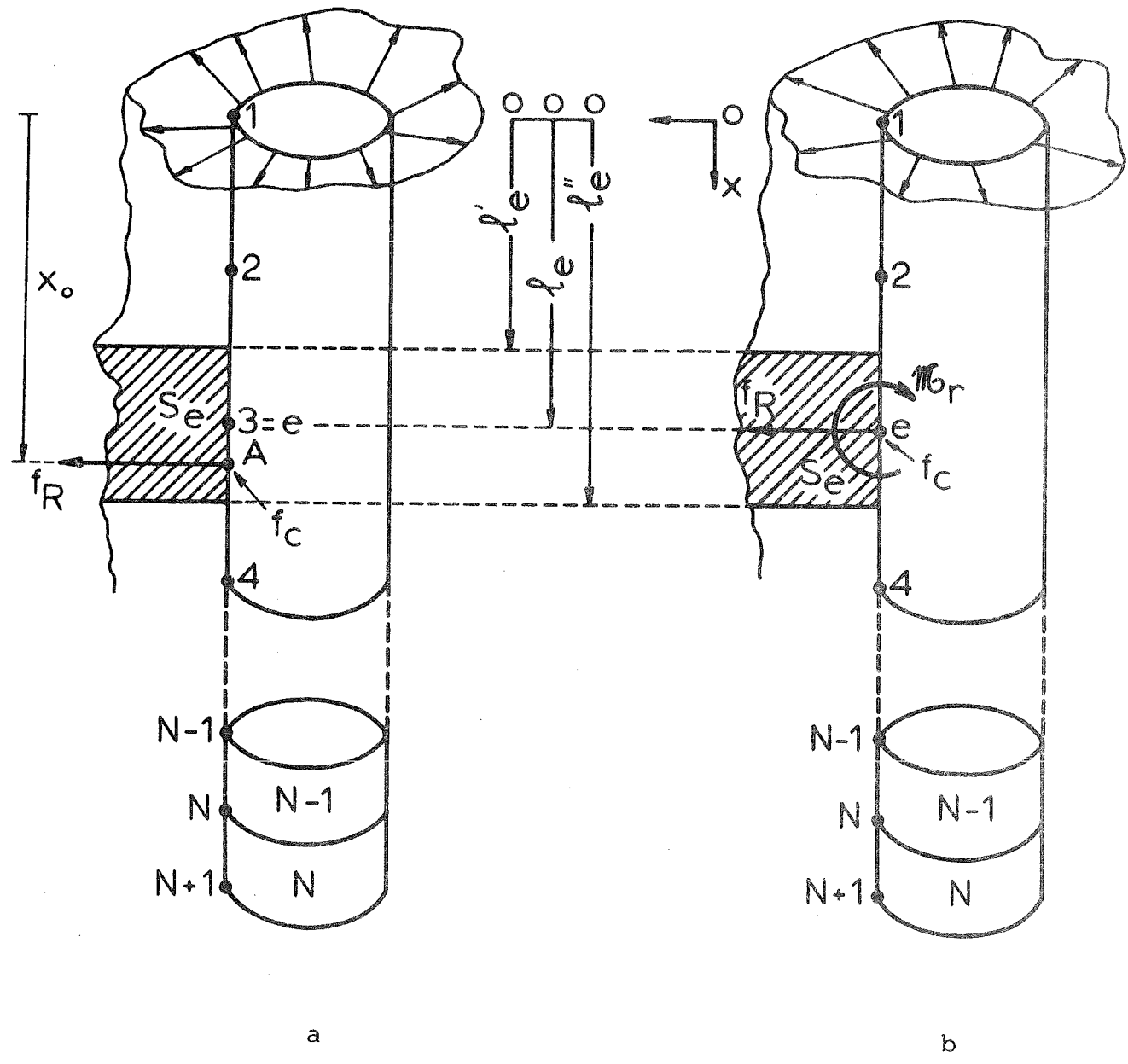
FIGURE 3 (a) Transformation of the continuous pressure field to a discrete force field

(b) The equivalent discrete force field acting at the node, e, involving f_R, f_C and $\mathcal{M}_r$.
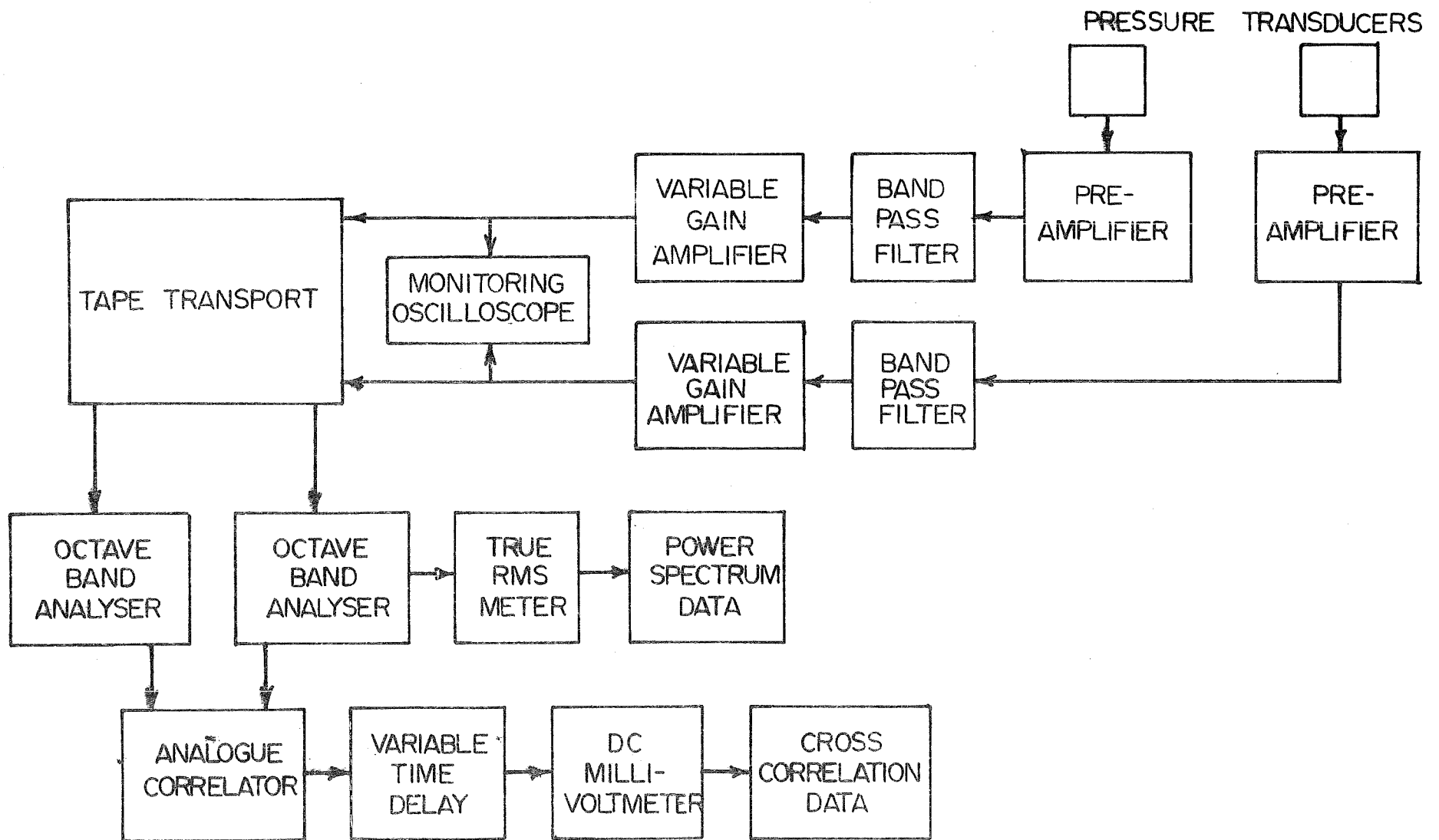
FIGURE 4   Block diagram of instrumentation used for recording and analyzing turbulent wall-pressure field.
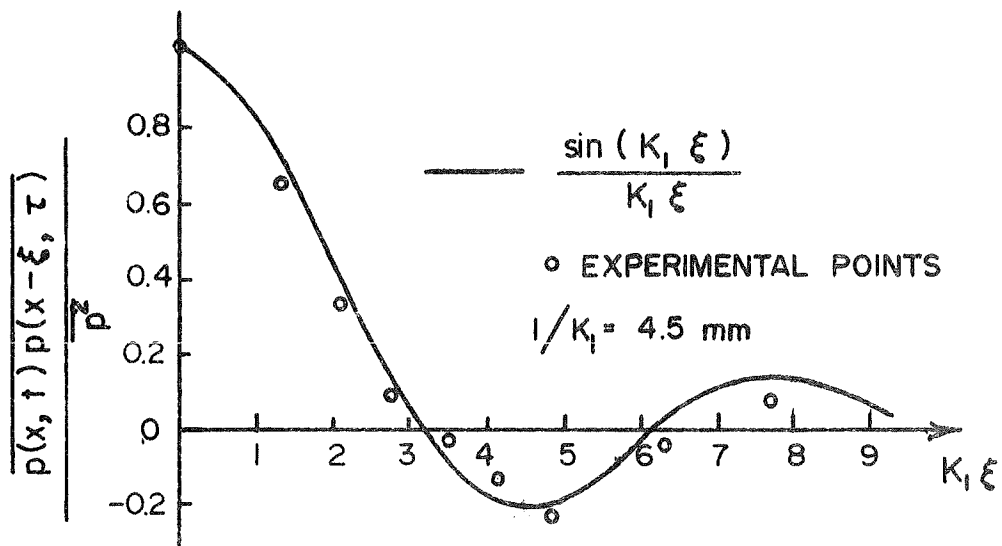
(a)
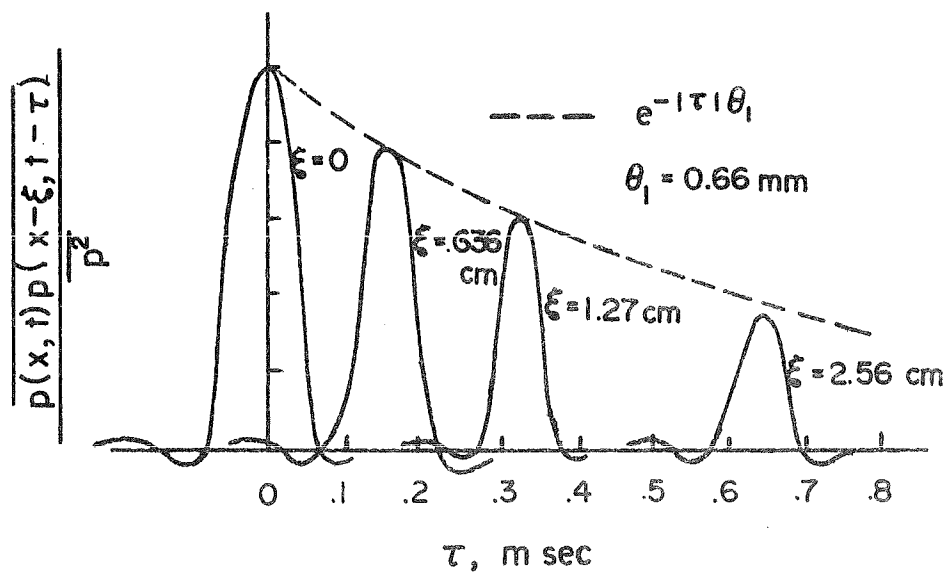
(b)

FIGURE 5 a) Longitudinal spatial pressure correlations at
            U_∞ = 40 m/sec and a frequency of 450 Hz.

         b) Longitudinal space-time pressure correlations at
            U_∞ = 40 m/sec and a frequency of 450 Hz.

(Reproduced of Tack et al. [35], Figures 1 and 2).
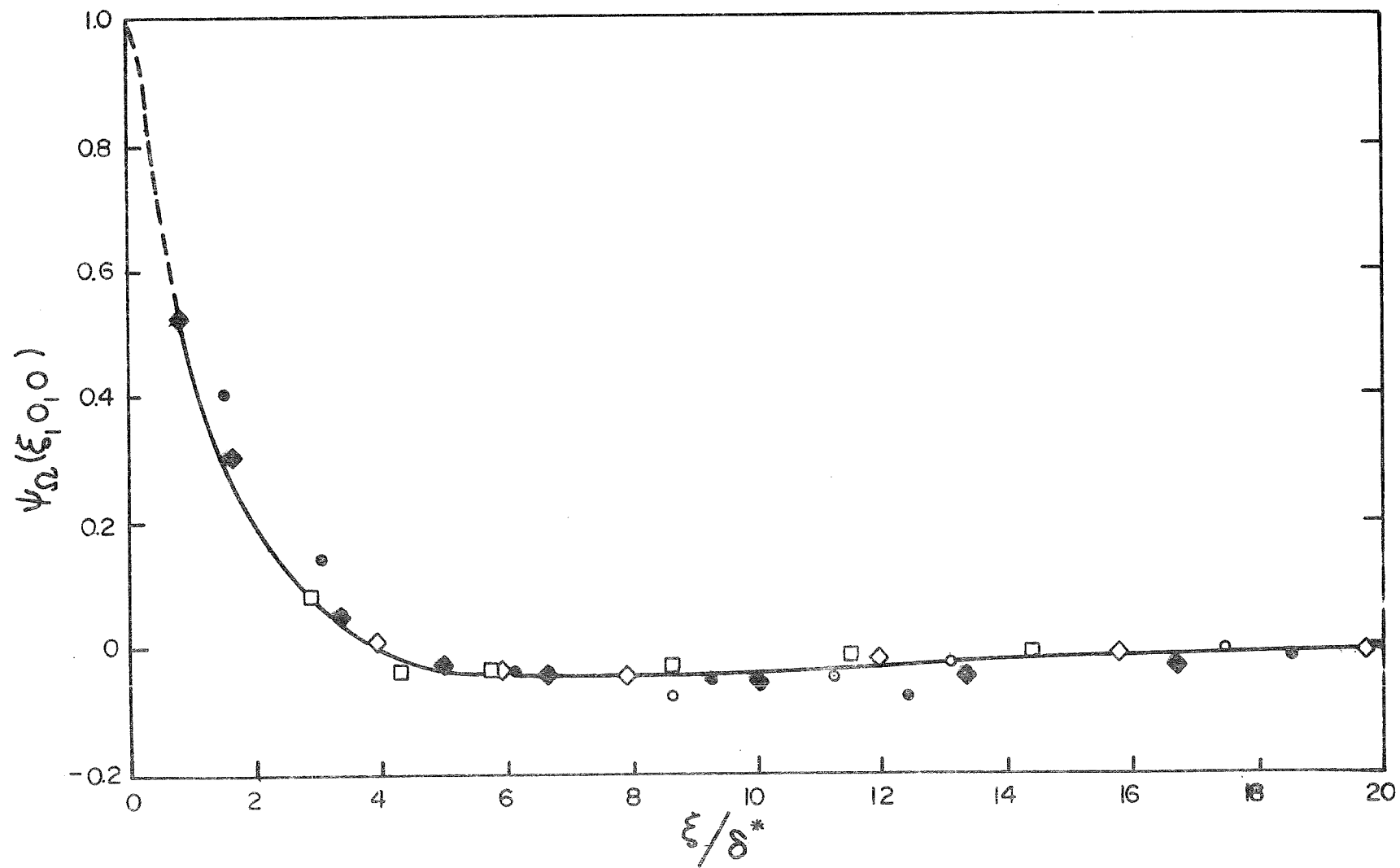
FIGURE 6a Longitudinal space correlation of the wall-pressure field, Ψ_Ω $(\xi, 0, 0)$
(Reproduced of Bull [36], Figure 9).
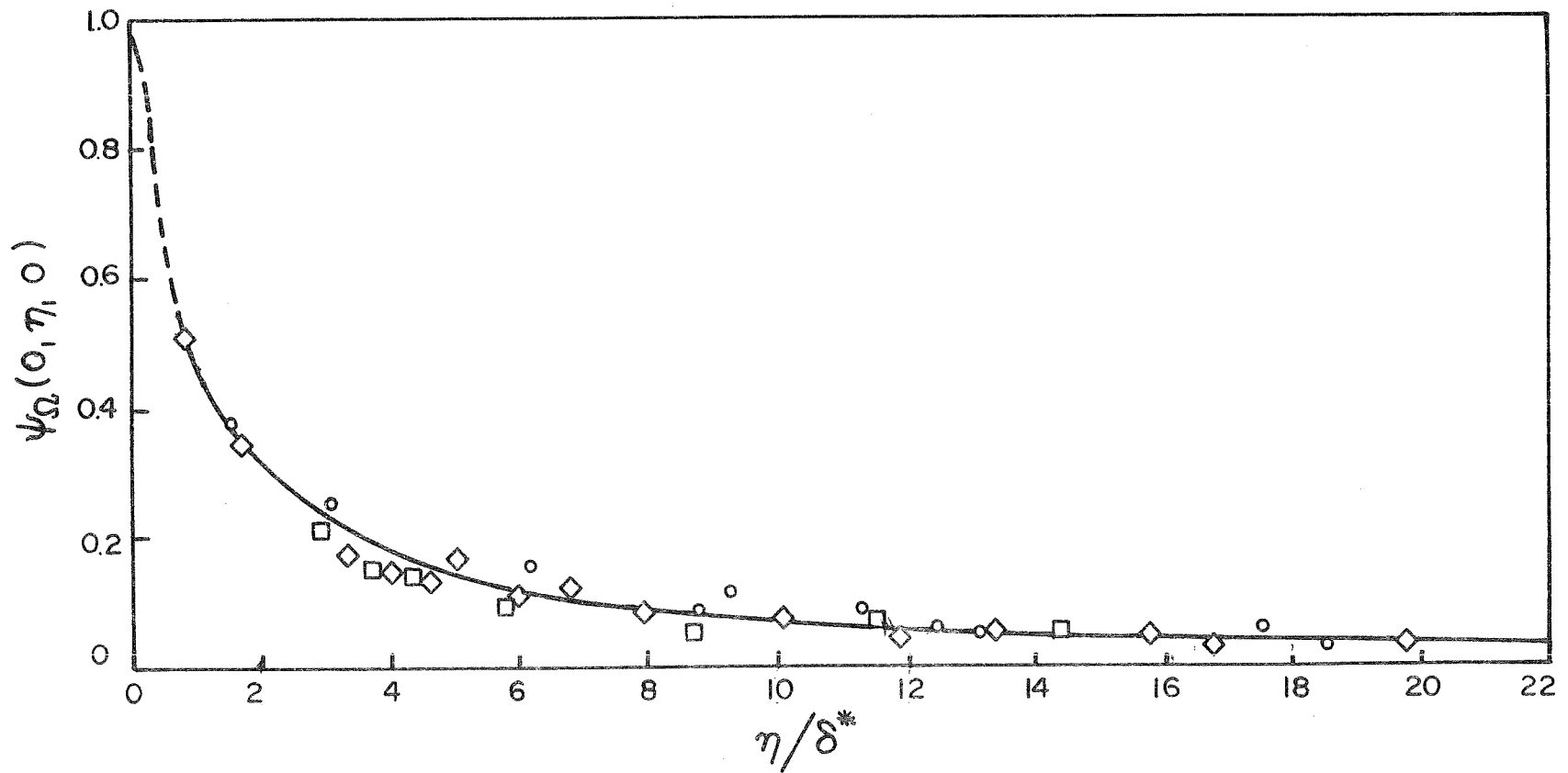
FIGURE 6b Lateral space correlation of the wall-pressure field, Ψ_Ω (0, η, 0);
$\delta^*$is the boundary-layer thickness.

(Reproduced of Bull [36], Figure 10).
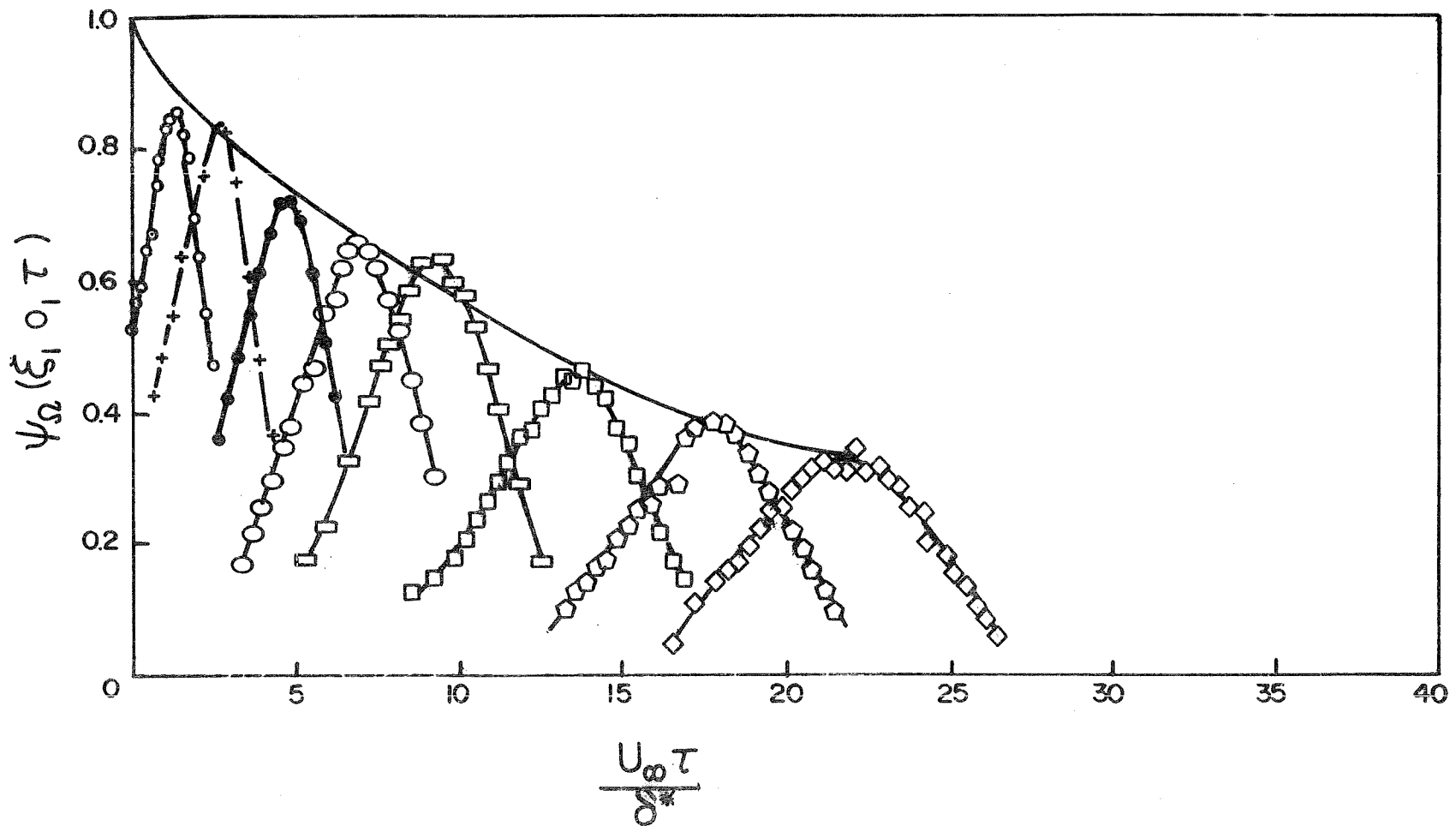
FIGURE 7 Peaks of curves of longitudinal space-time correlation, Ψ_Ω $(\xi, 0, \zeta)$

$M_0 = 0.3$, $\delta^* = 0.149$ inch $X = 87.6$ inches

M_0 is the mach number, δ^*, boundary-layer thickness, x, axial coordinate and

ζ is the time delay.

(Reproduced of Bull [36], Figure 13).

FIGURE 8 Frequency spectrum of wall-pressure fluctuations; where q_∞ is the free-stream pressure, Ω, the central frequency; δ^*, boundary-layer thickness and U_∞ is the centerline velocity. (Reproduced of Bull [36], Figure 7).
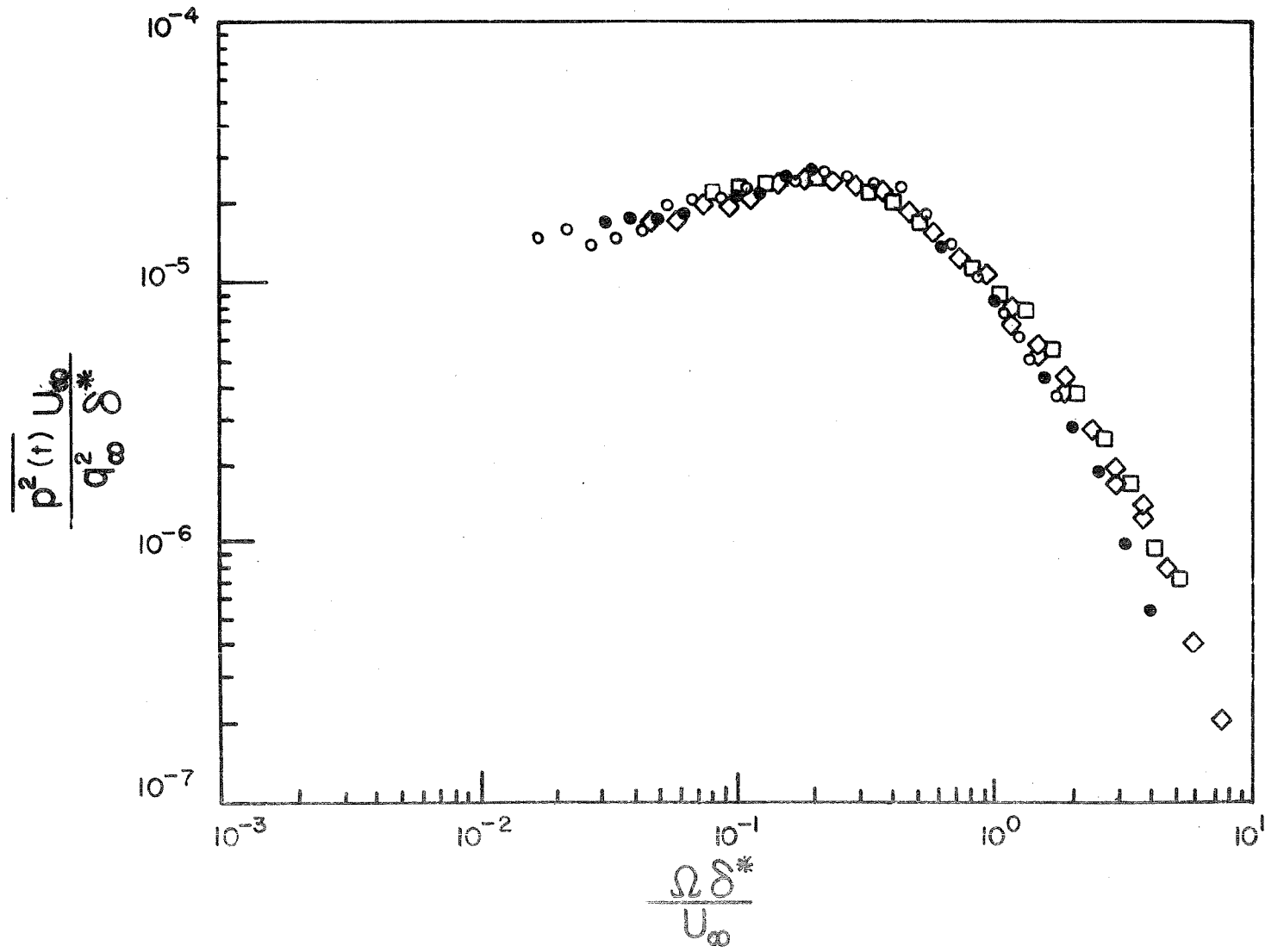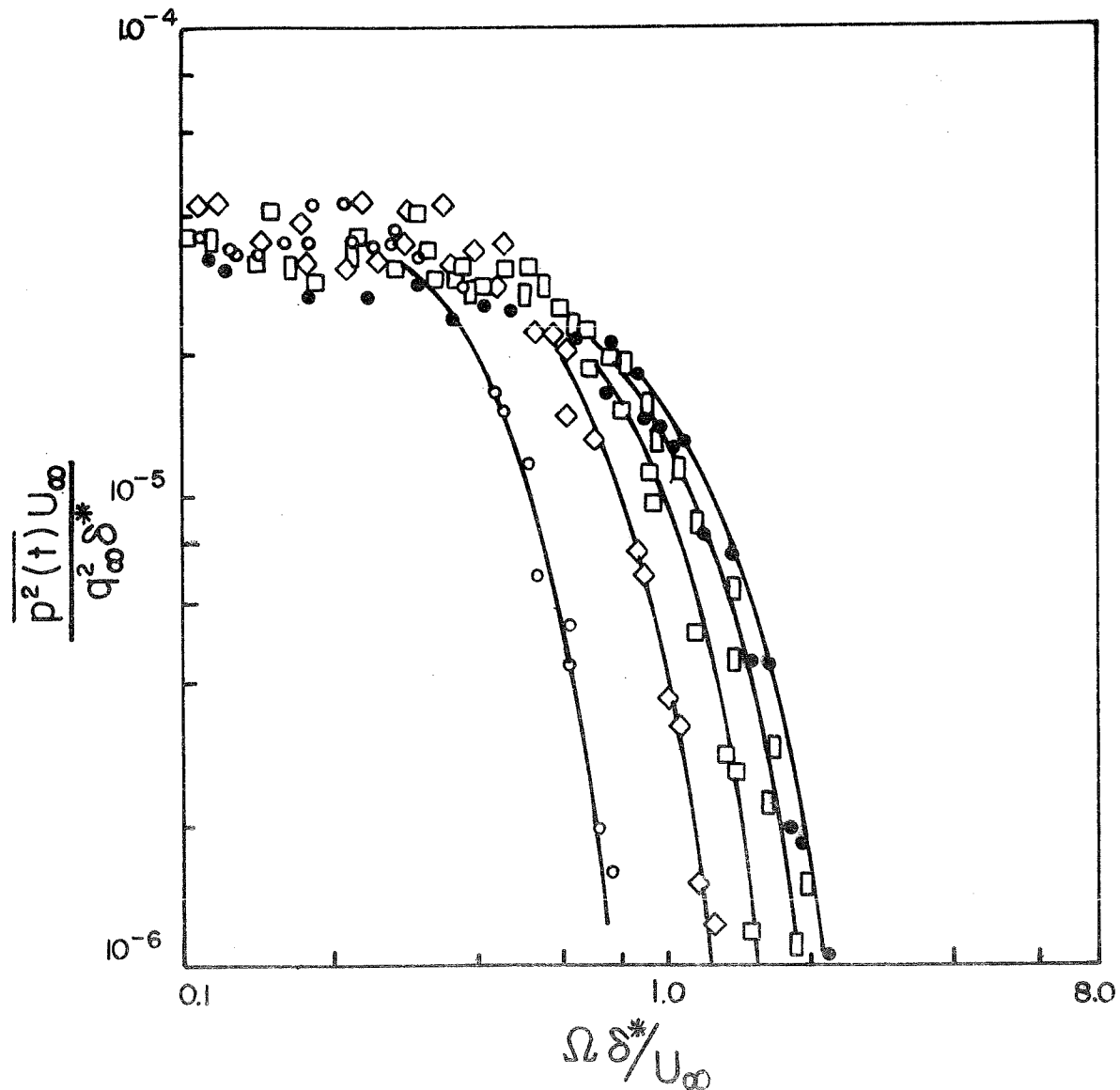
FIGURE 9 Power spectra of fluctuating wall pressure in a turbulent boundary layer; q_∞ is the free-stream pressure, Ω, the central frequency; δ^*, boundary-layer thickness and U_∞ is the centerline velocity.

(Reproduced of Willmarth [43], Figure 6).
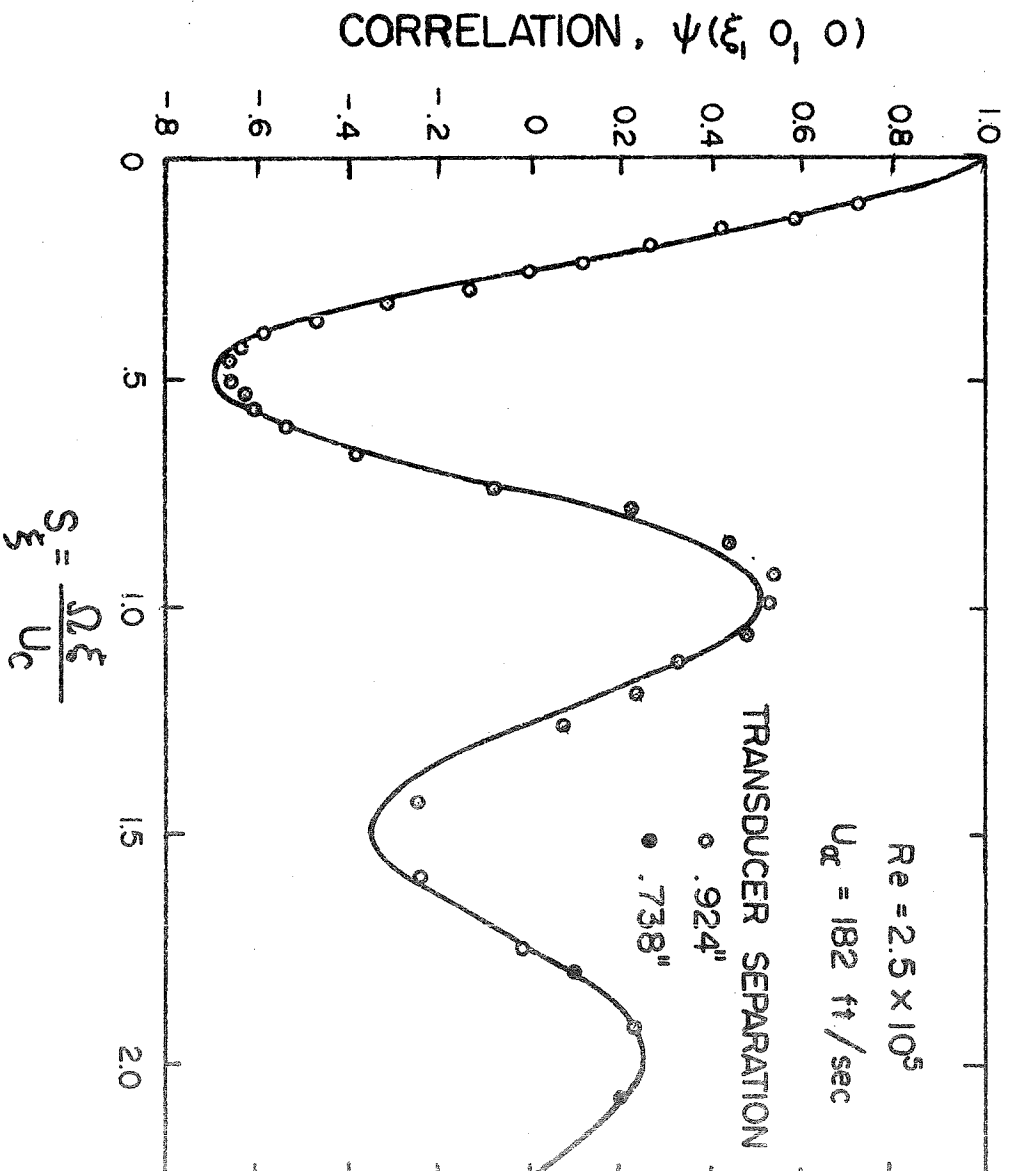
FIGURE 10 Longitudinal correlation versus Strouhal number based
on convection velocity (U_{CONV}).
(Reproduction of Bakewell [44], Figure 3.
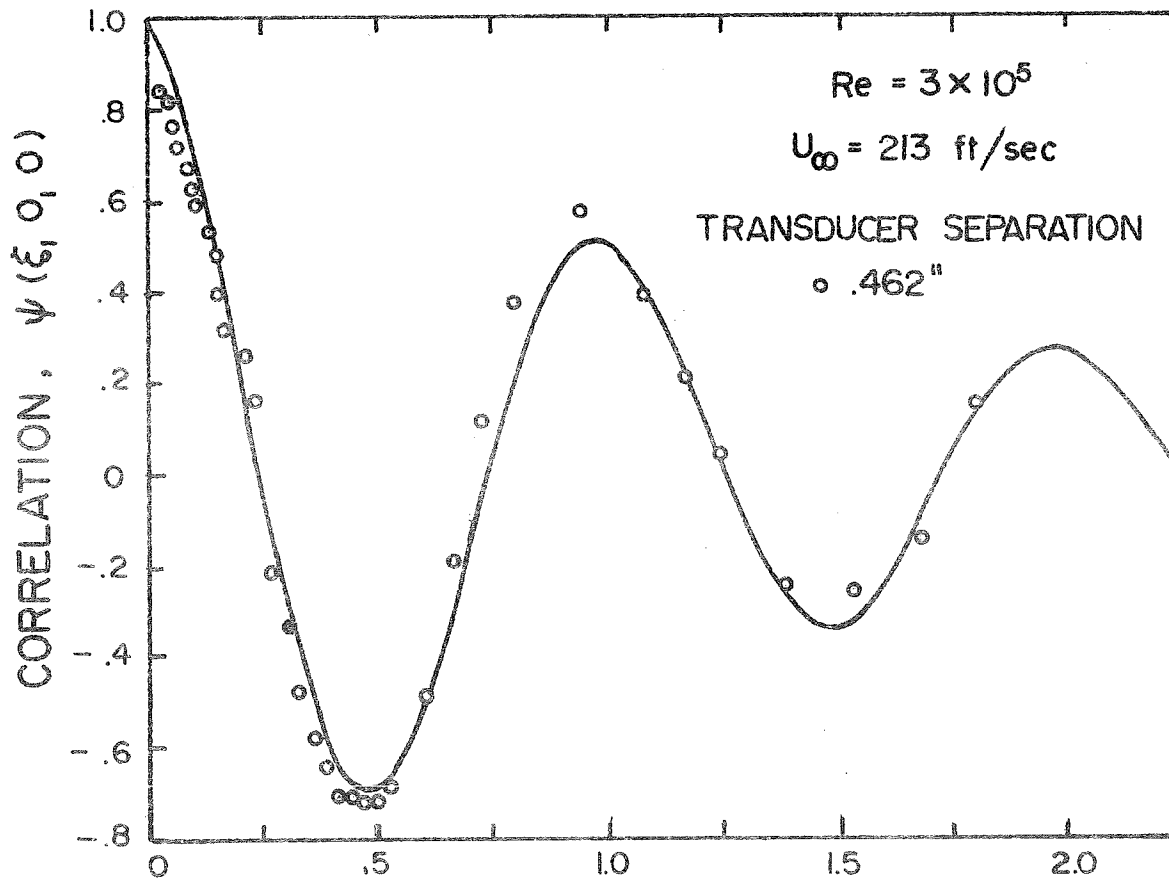
FIGURE 10 (Cont.) Longitudinal correlation versus Strouhal number based on convection velocity (U_{CONV}).

(Reproduction of Bakewell [44], Figure 4.
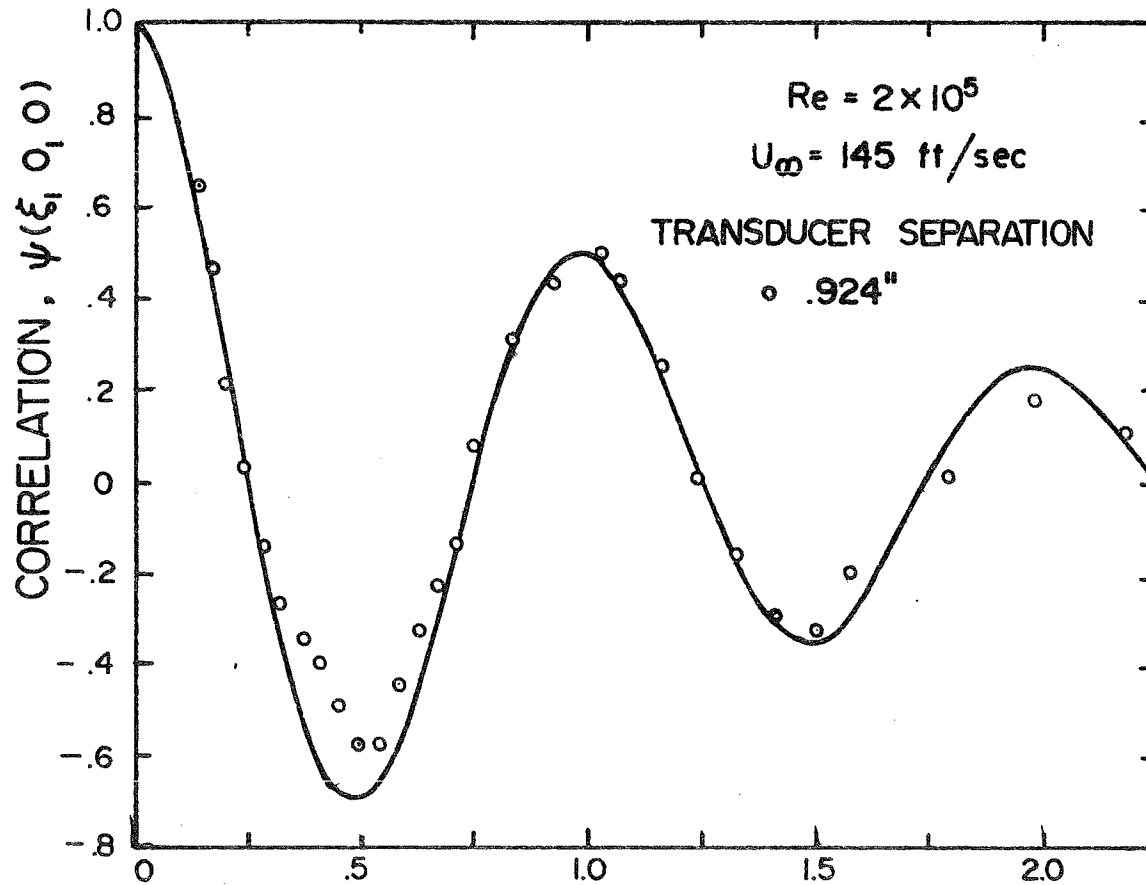
FIGURE 10 (Cont.)   Longitudinal correlation versus Strouhal number
based on convection velocity (U_{CONV}).

(Reproduction of Bakewell [44], Figure 5.
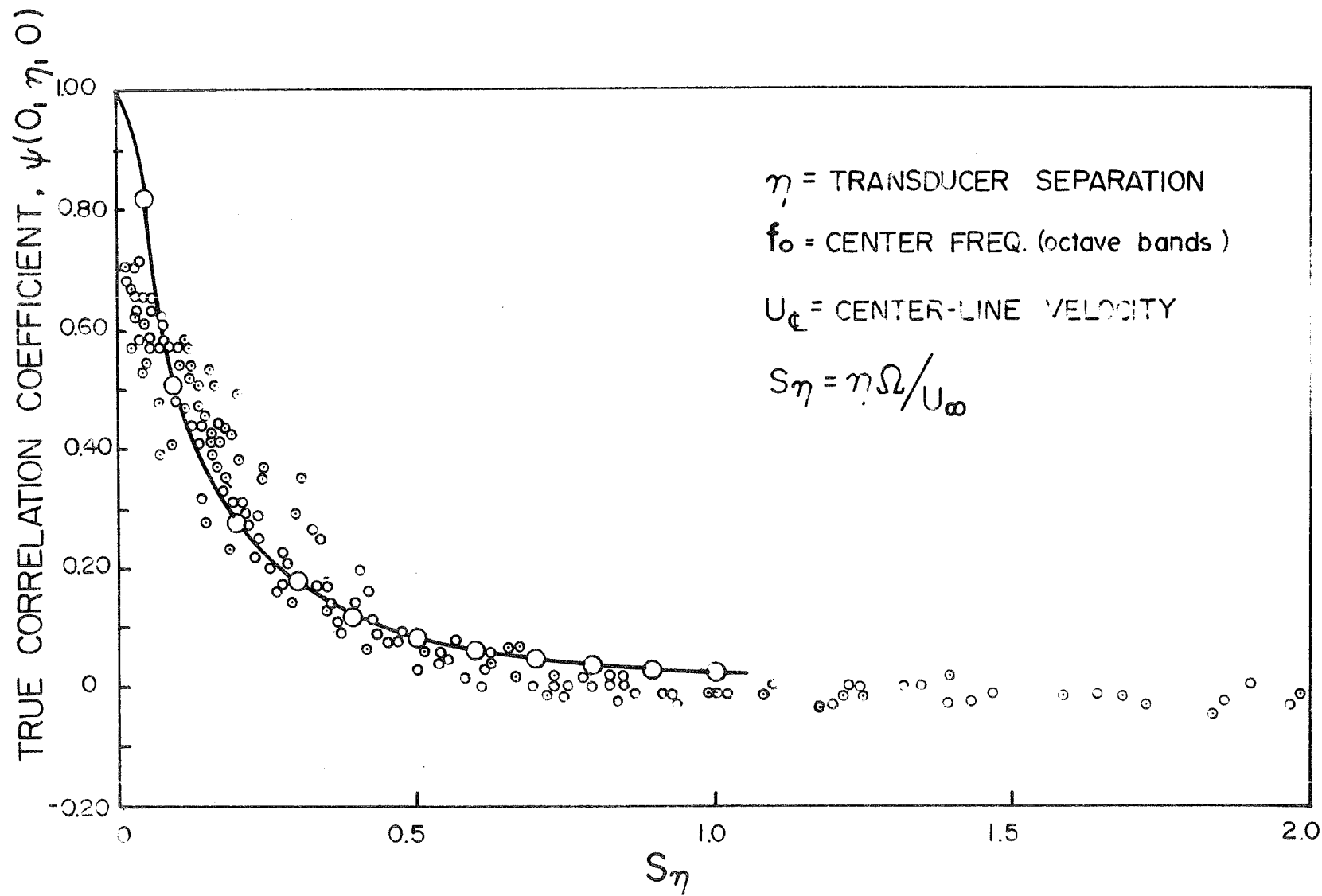
FIGURE 11 Lateral correlation versus Strouhal number based on centerline velocity.
(Reproduction of Bakewell [46], Figure 30).
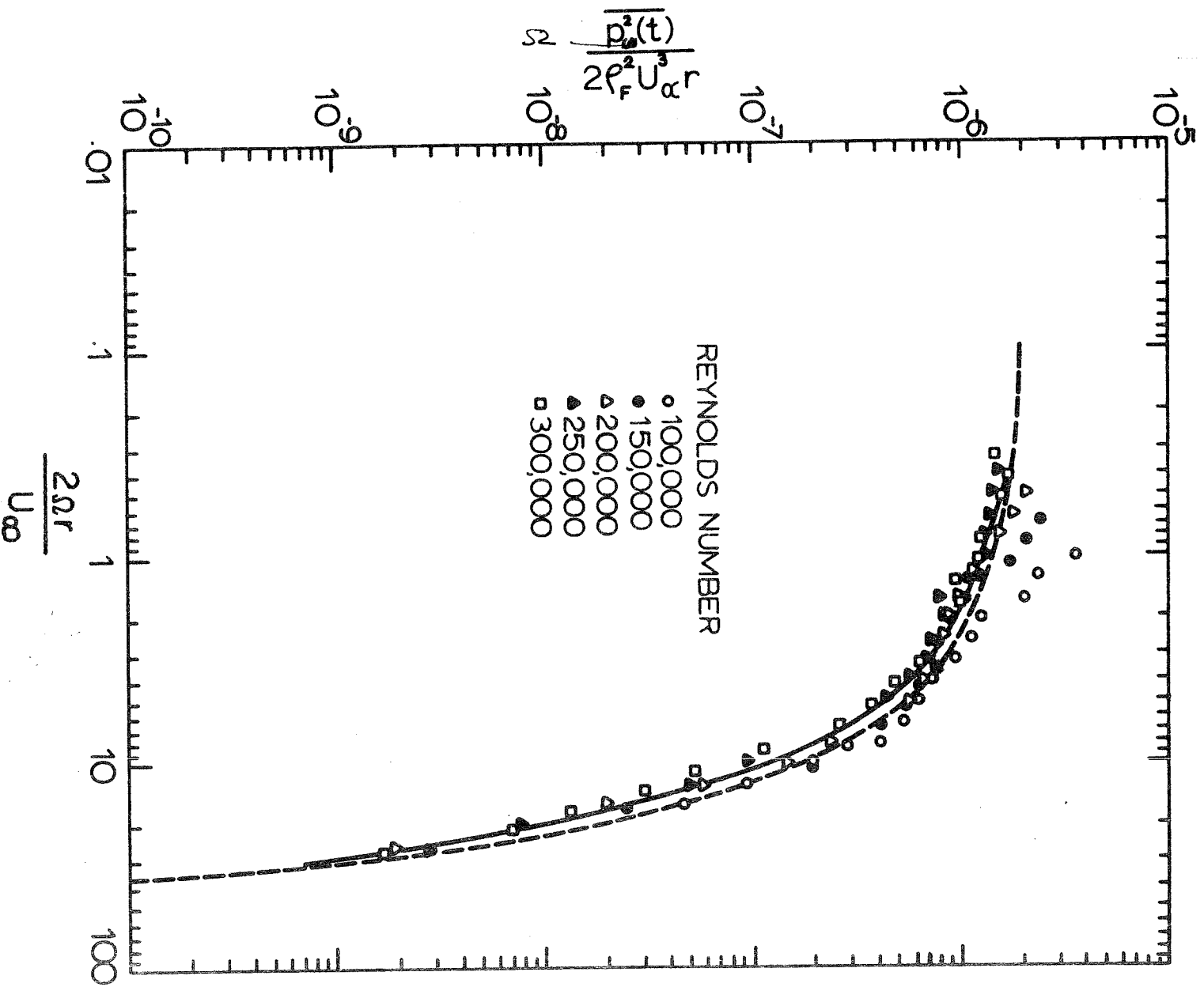
FIGURE 12 Bakewell's measurements [46] of the mean square pressure
per unit band-width, compared with the expression
used in this theory. _____ Bakewell's line of best
fit; _ _ _ _ equation (16) of this paper.

75
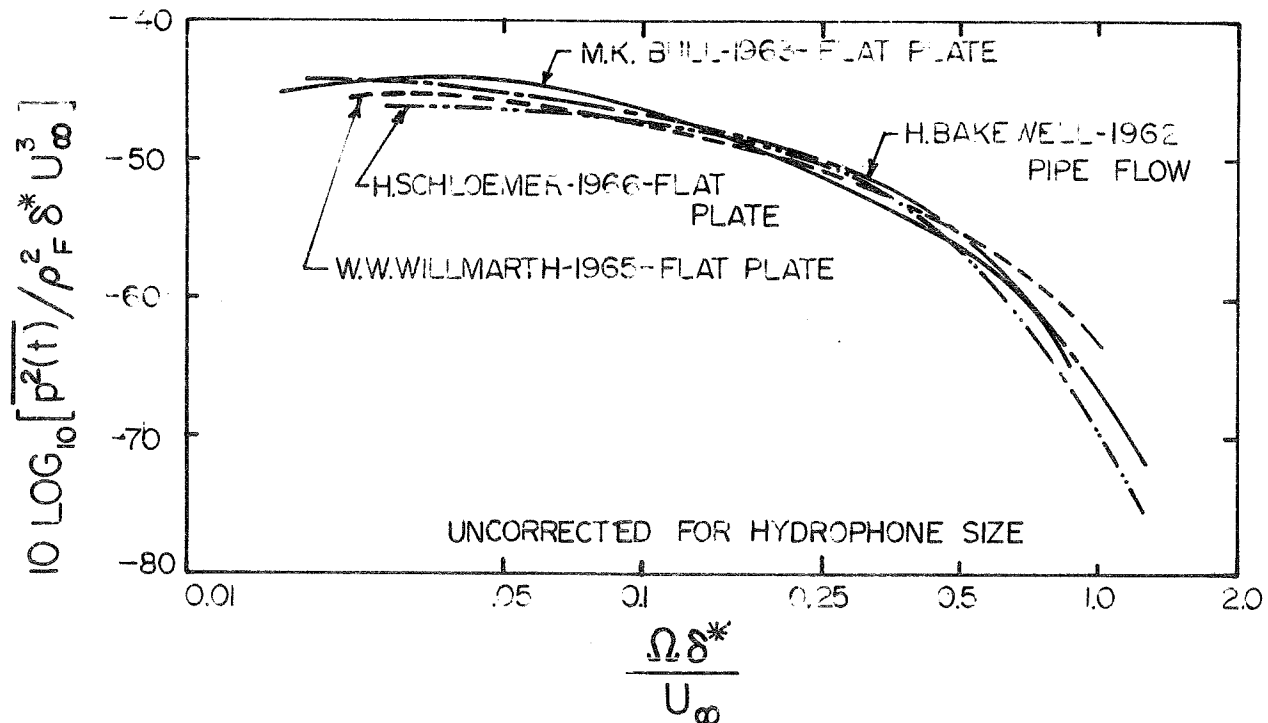
FIGURE 13 Nondimensional spectral density for zero pressure gradient compared with results of other investigators.

(Reproduced of Schloemer $\begin{bmatrix} 38 \end{bmatrix}$, Figure 10).
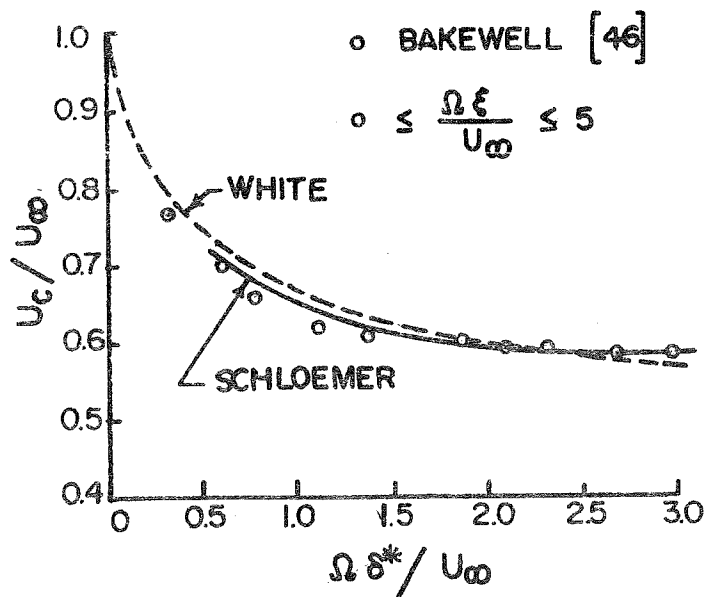
FIGURE 14   Convection velocity.

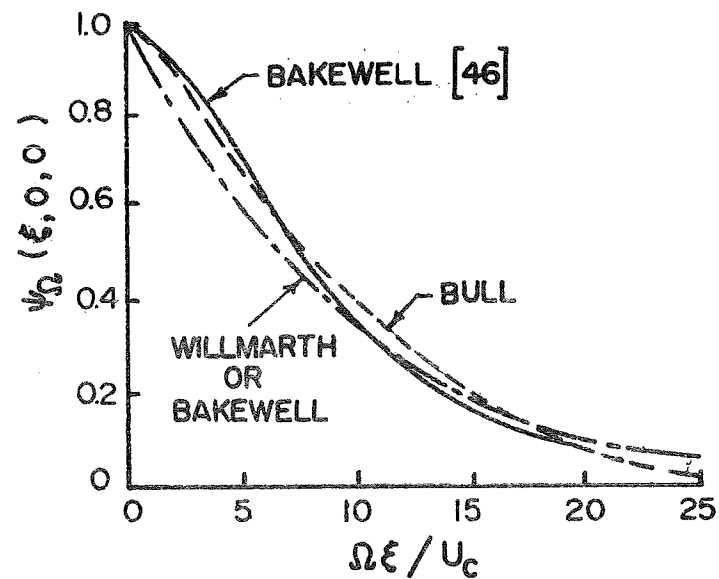(Reproduced of Bakewell $\left[42\right]$, Figure 7.

FIGURE 15   Magnitude of the longitudinal
cross-spectral density.

(Reproduced of Bakewell $\left[42\right]$, Figure 8.
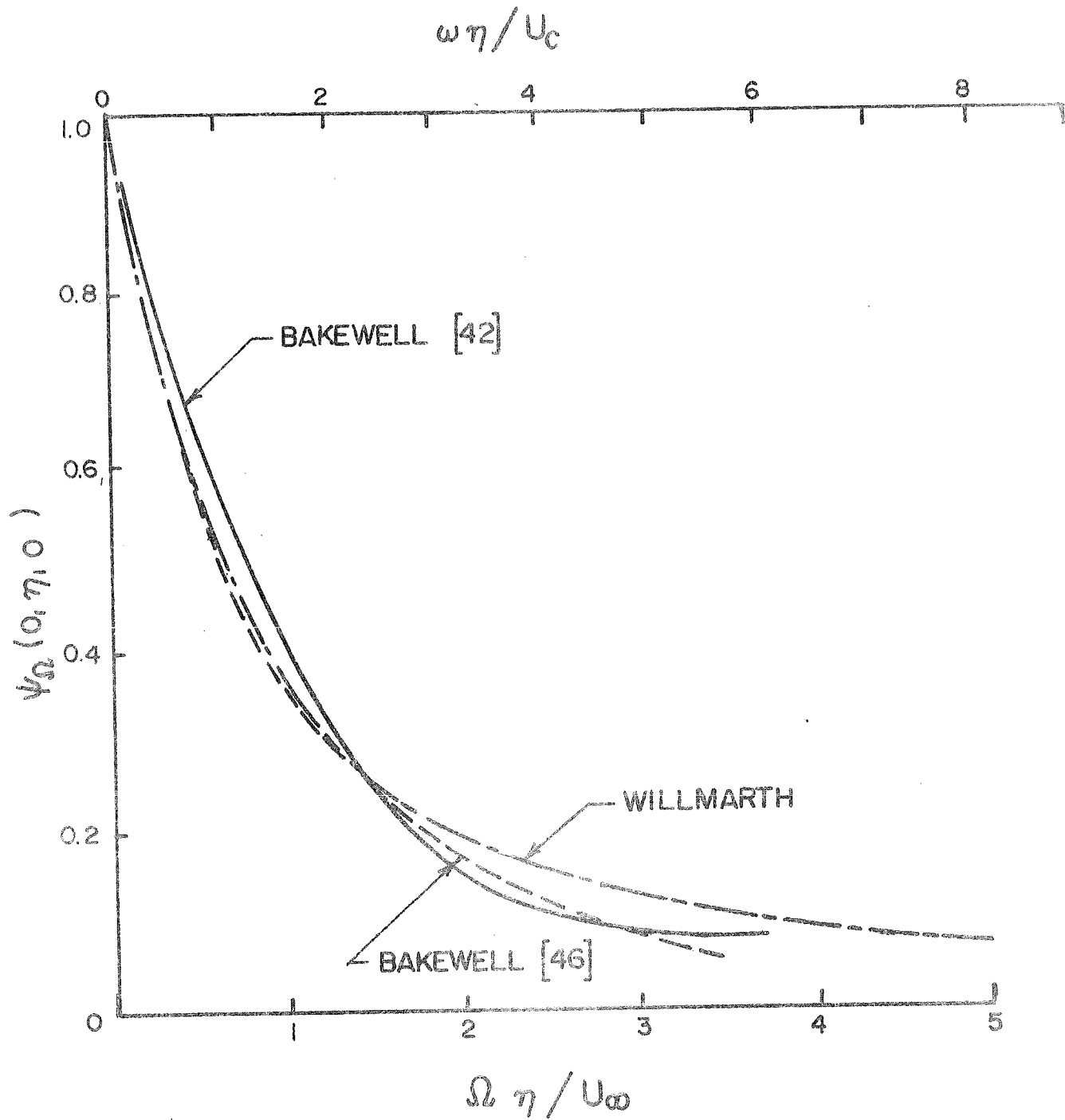
FIGURE 16 Magnitude of the lateral cross-spectral density.
(Reproduced of Bakewell [42], Figure 9.